

# DEEP ORDER FLOW IMBALANCE: EXTRACTING ALPHA AT MULTIPLE HORIZONS FROM THE LIMIT ORDER BOOK

PETTER N. KOLM, JEREMY TURIEL AND NICHOLAS WESTRAY

Petter N. Kolm is Clinical Professor and Director of the Mathematics in Finance  
Master's Program at NYU's Courant Institute of Mathematical Sciences, New  
York, NY 10012  
*petter.kolm@nyu.edu*

Jeremy D. Turiel is Ph.D. Candidate at University College London, Department  
of Computer Science, 66-72 Gower Street, London WC1E 6EA  
*jeremy.turiel.18@ucl.ac.uk*

Nicholas Westray is Visiting Researcher in Financial Machine Learning at NYU's  
Courant Institute of Mathematical Sciences, New York, NY 10012  
*nicholas.westray@nyu.edu*

**ABSTRACT.** We employ deep learning in forecasting high-frequency returns at multiple horizons for 115 stocks traded on Nasdaq using order book information at the most granular level. While raw order book states can be used as input to the forecasting models, we achieve state-of-the-art predictive accuracy by training simpler “off-the-shelf” artificial neural networks on stationary inputs derived from the order book. Specifically, models trained on order flow significantly outperform most models trained directly on order books. Using cross-sectional regressions we link the forecasting performance of a long short-term memory network to stock characteristics at the market microstructure level, suggesting that “information-rich” stocks can be predicted more accurately. Finally, we demonstrate that the effective horizon of stock specific forecasts is approximately two average price changes.

## 1. INTRODUCTION

In this article we employ deep learning (DL) in forecasting high-frequency returns at multiple horizons for 115 stocks traded on Nasdaq using order book information at the most granular level. In the last decade, DL has experienced enormous success, outperforming more traditional approaches in areas such as image classification, computer vision and natural language processing (Krizhevsky et al., 2012; LeCun et al., 2015; Schmidhuber, 2015; Goodfellow et al., 2016; Devlin et al.,

---

*Date:* August 6, 2021.

*Key words and phrases.* Artificial neural networks; Deep learning; Financial machine learning; High-frequency trading; Limit order books; Market microstructure; Multiple horizons; Order flow; Return predictability.

2018). A key reason for this success is that DL learns suitable representations directly from the raw data, unlike conventional machine learning (ML) approaches where features are designed by hand and frequently involve domain expertise. Artificial neural networks (ANNs) have proven to be particularly good at extracting intricate relationships in complex and high-dimensional settings *without* human input, especially when trained on large amounts of raw data. Although counterintuitive from the perspective of traditional statistical and ML techniques, where the researcher uses handcrafted features and progresses from simpler to more complex models, the essence of DL and related approaches is eloquently summarized in the following quote by Rich Sutton: “The biggest lesson that can be read from 70 years of AI research is that *general methods that leverage computation* are ultimately the most effective, and by a large margin.” (emphasis added) (Sutton, 2019).

While results have been mixed because of the lack of enough data, ANNs have been applied to a number of problems in finance (see, for example, the surveys by Wong et al. (1998), Li et al. (2010), Elmsili et al. (2018), Ozbayoglu et al. (2020), and Sezer et al. (2020)). Recently, by leveraging large datasets extracted from limit order books (LOB) in equity markets, ANNs have been successful at forecasting high-frequency returns (see, for example, Tsantekidis et al. (2017), Tran et al. (2019), Zhang et al. (2018), Sirignano (2019), Sirignano et al. (2019), Zhang et al. (2019a), Zhang et al. (2019b), Luo et al. (2019), Tsantekidis et al. (2020), Briola et al. (2020), Zhang et al. (2021a), and Zhang et al. (2021b)).

The literature to date has focused on two key empirical questions. First, to demonstrate that deep learning models outperform classical statistical and machine learning approaches, including penalized linear models, decision trees and kernel-based models. Second, to identify the optimal ANN architecture for return classification. While the answer to the first question has been established in favor of ANNs, the choice of the optimal ANN architecture is less clear.

The most common ANNs in these studies are convolutional neural networks (CNNs), long short-term memory networks (LSTMs), multilayer perceptrons (MLPs), or a combination thereof.<sup>1</sup> For example, Tsantekidis et al. (2017) and Tsantekidis et al. (2020) and Zhang et al., 2019a advocate for CNNs, in the latter case with an additional *inception module* (Szegedy et al., 2015). In contrast, Sirignano et al. (2019) provide evidence in favor of stacked LSTMs, and the horse race conducted by Briola et al. (2020) suggests that, as a universal function approximator, a large enough MLP performs as well as the CNN-LSTM of Zhang et al. (2018), an ANN where an LSTM layer is applied to the time series output of a CNN. Additionally, Tsantekidis et al. (2020) compare a CNN, LSTM and CNN-LSTM. They find their

<sup>1</sup>See the textbooks by Goodfellow et al. (2016) and Friedman et al. (2017) for an introduction to DL and a discussion of many of the standard ANN architectures.

CNN-LSTM leads to more stable behaviour and outperforms their other models. By combining bilinear projection and an attention mechanism (Bahdanau et al., 2014; Mnih et al., 2014), Tran et al. (2019) propose a temporal attention-augmented bilinear network architecture for mid-price return classification and show it outperforms a CNN, LSTM, and MLP on their dataset. Passalis et al. (2020) develop a temporal logistic neural bag-of-features model that feeds into an MLP, demonstrating that it performs better than their benchmark models (including a CNN, GRU<sup>2</sup>, LSTM, and MLP) in determining whether the mid-price will increase, decrease, or remain the same.

In the majority of these studies, model inputs are represented as raw or transformed time series of order book states (one major exchange is chosen in the case of fragmented markets) and the return forecasting problem is formulated as a *classification task*, where a single forecasting horizon is chosen to be either a deterministic time interval such as two seconds, or a stochastic time interval such as until the next price change. A notable exception is the work of Mäkinen et al. (2019) that forecasts the arrival of jumps in one-minute ahead stock returns. In a recent article, Rahimikia et al. (2021) examine the performance of forecasting realized volatility with LSTMs using order book data from LOBSTER and news sentiment derived from Dow Jones Newswires.

The objective of the classification frameworks in the literature is to predict the sign of the return over the specified horizon (two classes), or whether prices will go up, down or not change (three classes). The most common approach to create class labels is by smoothing forward prices using moving averages over some prespecified forecast horizon, and then to assign labels based on thresholding. While these labeling methods provide a form of regularization by removing noise, they introduce ad hoc modeling parameters that are undesirable in real-world trading applications. In particular, with the exception of special cases, there is no canonical way to perform such labeling.

As most studies use different datasets, direct comparison of the model architectures is challenging. Indeed, it may well be the case that there is no one single “optimal architecture” and different datasets warrant distinct ANNs. Most articles rely on the FI-2010 benchmark dataset of Ntakaris et al. (2018) that consists of ten days of limit order book events for five companies traded on the Nasdaq Nordic exchange. Notably, the FI-2010 dataset is downsampled and does not represent the limit order books of the stocks at the most granular level as the data has been

---

<sup>2</sup>The *gated recurrent unit* (GRU) was introduced by Cho et al. (2014). See also Jozefowicz et al. (2015) who compare the performance of the GRU and LSTM on a number of standard benchmark problems.

preprocessed following the procedure described in (Kercheval et al., 2015). In addition, with a smaller dataset it is not obvious that results will generalize to other stocks, exchanges and/or time periods. Sirignano et al. (2019) employ the most comprehensive dataset to date, assembled from LOBSTER (Huang et al., 2011), consisting of order book events of about 1000 stocks traded on the Nasdaq from January 1, 2014 through March 31, 2017. In this study, using a stacked LSTM with three layers, the authors provide compelling evidence for a universal relationship between order book states and price changes. In a related article, with a similar dataset consisting of 489 symbols from the S&P 500 and Nasdaq 100 over the period January 1, 2014 through August 31, 2015, Sirignano (2019) proposes a new spatial neural network architecture and demonstrates that this outperforms logistic regression and an MLP in the return classification task.

The present article makes four main contributions to the literature on high-frequency return forecasting in limit order books. First, in contrast to the previous literature, we formulate the forecasting problem as one of regression to avoid issues associated with that of training classifiers. Unlike the most common regression setup where the forecast is a scalar, we deploy a *multi-output regression framework* where the model for each stock outputs a vector we refer to as an *alpha term structure*. Each element of the alpha term structure represents a mid-price return forecast at a specified horizon. Alpha term structures render representations of the timescales over which alpha may rise and/or decay that are very useful in real-world trading. For instance, they can be used in designing order placement strategies in optimal execution and market making, and other high-frequency trading strategies. In addition, contrary to many previous studies that use classification, our regression setup obviates the need for any smoothing of the dependent variables.

Second, we perform a large-scale forecasting horse race with common ANNs, including an MLP, LSTM, LSTM-MLP, stacked LSTM and CNN-LSTM, trained on different inputs including limit order book states for the first ten (non-zero) levels and data derived from the order book. Besides our CNN-LSTM, that is similar in spirit to the architecture used by Zhang et al. (2018), all other models are standard “off-the-shelf” ANNs. Sourced from LOBSTER, our dataset consists of order book events timestamped to nanosecond precision for 115 Nasdaq stocks for the period January 1, 2019 through January 31, 2020. In contrast to many previous studies, we do not downsample our data but work directly with the raw limit order book states. We demonstrate that while limit order book states, which are a complex *non-stationary* multivariate process, can be used directly as inputs for the ANN models, forecasting performance can be improved significantly by training the models on *stationary* inputs. In particular, we show that ANNs trained on *order*

*flow*, stationary quantities derived from the limit order book (Cont et al., 2014), significantly outperform most models that are trained directly on order book states.

Third, using cross-sectional regressions we link the forecasting performance of the LSTM model to stock characteristics at the market microstructure level. We show that “information-rich” stocks, defined as stocks that have a higher number of order book updates per price change, can be forecasted more accurately by DL models.

Fourth, by leveraging the multi-output regression setup we analyze the shape of the alpha term structure from the models. Specifically, we show that stock-level alphas peak at a time scale of about two price changes and decline thereafter. Notably, in their recent work, Zhang et al. (2021b) deploy a multi-horizon design. However, they use a classification setup and their Seq2Seq architecture of Cho et al. (2014) is quite different from the ANNs we use.

The outline of the article is as follows. In Section 2 we review the mechanics of limit order book markets and specify the forecasting models used in this study. We describe our data, its preprocessing, and our forecasting and model evaluation methodology in Section 3. We present our empirical results and findings in Section 4. Section 5 concludes.

## 2. PRELIMINARIES

In Section 2.1, we provide an introduction to limit order books, their representation in full and reduced-form, including order book states (LOB), order flow (OF), and order flow imbalance (OFI). Then in Section 2.2, we describe the forecasting models used in this study, including an autoregression with exogenous inputs (ARX), multilayer perceptron (MLP), long short-term memory (LSTM), LSTM-MLP, stacked LSTM, and CNN-LSTM. The first model is a classical linear model whereas the last five are ANN architectures.

**2.1. Limit Order Books and Order Flow.** Modern equity trading is conducted electronically. Major exchanges in the U.S. and the rest of the world facilitate this via a *limit order book* (or *order book*, for short), one per stock. The order book represents a collection of buyers and sellers, ordered by price and time, bidding and offering stock for purchase or sale. Figure 1 depicts an order book where buyers and sellers are shaded in blue and yellow, respectively.

At a given time  $t$ , the highest price buyers are prepared to buy the stock for is called the *bid price* and is denoted by  $b_t$ . Similarly, the lowest price sellers are prepared to sell the stock for is referred to as the *ask price* and is denoted by  $a_t$ . From the limit order book, we can derive the *mid-price*,  $p_t := (b_t + a_t)/2$ , the *bid-ask spread*,  $a_t - b_t$ , and the *tick size*, the smallest price increment between different

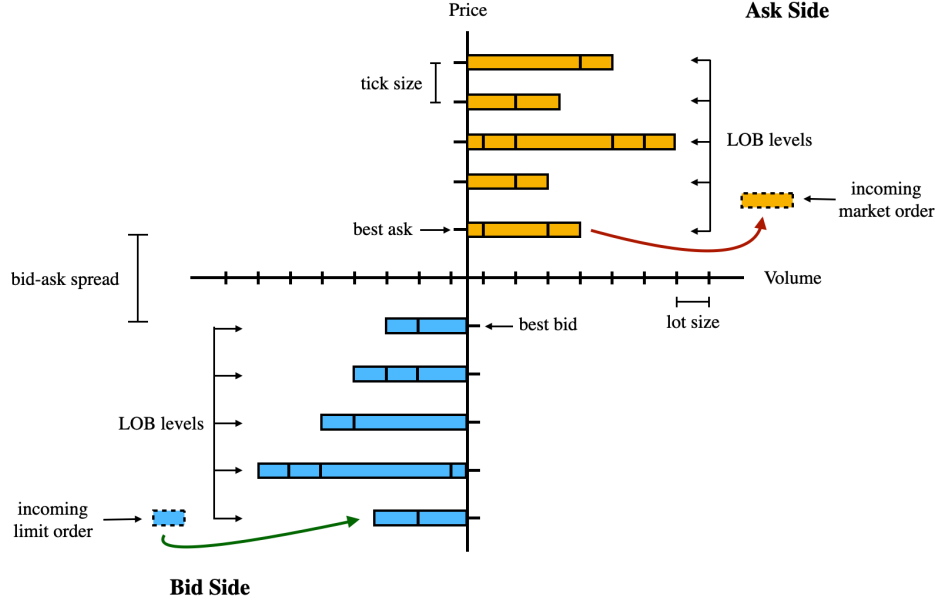


FIGURE 1. An illustration of a limit order book. We observe a market order being filled at the ask side and an incoming limit order being added to the bid side.

price levels in the order book, as illustrated in Figure 1. For the Nasdaq exchange, which is the focus of this article, the tick size is \$0.01. Beyond the bid and ask, there are additional *levels* in the order book.

An *order* is defined as the four-tuple (side, quantity, price, time), representing the side of the order book the order is posted to, the price at which the order is submitted, the desired amount to be traded and the time of submission. Orders may be entered, and if active, cancelled at any time. When an order is submitted the matching engine of the exchange attempts to match it with existing orders in the book. Orders which match are called *market orders*. Orders which do not match, or only match partially, are referred to as a *limit orders*. When there are multiple limit orders with the same side and price present, they are queued chronologically at that price level according to the first-in-first-out (FIFO) principle. For an in-depth description of modern equity trading and the order book we refer to Gould et al. (2013), Abergel et al. (2016), and Bouchaud et al. (2018).

**2.1.1. Order Book States.** Throughout the rest of the article, we consider the first ten levels of the order book for each stock. We define the *state of the order book at time  $t$*  as the vector of price and volume information for the top ten (non-empty) bid and ask levels

$$\mathbf{s}_t^{\text{LOB}} := (a_t^1, v_t^{1,a}, b_t^1, v_t^{1,b}, \dots, a_t^{10}, v_t^{10,a}, b_t^{10}, v_t^{10,b})^\top \in \mathbb{R}^{40}, \quad (1)$$

where  $b_t^i, a_t^i$  are the bid and ask prices at the  $i$ -th level at time  $t$  and  $v_t^{i,b}, v_t^{i,a}$  are the corresponding share volumes. With a slight abuse of terminology, in the following we refer to time series of order book states as the *limit order book* (LOB). Note that the LOB for each stock is an irregularly spaced time series.

**2.1.2. Bid-Ask Order Flow and Order Flow Imbalance.** For each stock and date, we let  $t \in \{1, \dots, T\}$  denote an enumeration of all order book updates on that day. Given two consecutive order book states for the stock at  $t-1$  and  $t$  of the form (1), we define the *bid order flows* (bOF) and *ask order flows* (aOF) at time  $t$  as the vectors  $\mathbf{bOF}_t, \mathbf{aOF}_t \in \mathbb{R}^{10}$ , where each component is given by

$$\mathbf{bOF}_{t,i} := \begin{cases} v_t^{i,b}, & \text{if } b_t^i > b_{t-1}^i, \\ v_t^{i,b} - v_{t-1}^{i,b}, & \text{if } b_t^i = b_{t-1}^i, \\ -v_t^{i,b}, & \text{if } b_t^i < b_{t-1}^i, \end{cases} \quad (2)$$

$$\mathbf{aOF}_{t,i} := \begin{cases} -v_t^{i,a}, & \text{if } a_t^i > a_{t-1}^i, \\ v_t^{i,a} - v_{t-1}^{i,a}, & \text{if } a_t^i = a_{t-1}^i, \\ v_t^{i,a}, & \text{if } a_t^i < a_{t-1}^i, \end{cases} \quad (3)$$

for  $i = 1, \dots, 10$ . By concatenating and subtracting the bid and ask order flows at time  $t$ , we obtain the *order flow* (OF)

$$\mathbf{OF}_t := \begin{pmatrix} \mathbf{bOF}_t \\ \mathbf{aOF}_t \end{pmatrix} \in \mathbb{R}^{20}, \quad (4)$$

and the *order flow imbalance* (OFI)

$$\mathbf{OFI}_t := \mathbf{bOF}_t - \mathbf{aOF}_t \in \mathbb{R}^{10}, \quad (5)$$

respectively. The nonlinear transformations represented by formulas (2), (3) and (5) have become a common approach to map the nonstationary time series of order book states to a stationary time series (Cont et al., 2014). Cont et al. (2014) establish a linear relationship between price changes and OFI at the first level of the order book, and Xu et al. (2018) and Kolm et al. (2021) extend this result to multilevel and cross-sectional OFIs. Order flow as defined in equation (4), which keeps the bid and ask sides separate, represents a modest generalization of OFI and offers any forecasting exercise greater flexibility. In particular, unlike OFI that weights bid and ask order flows equally, by using the non-differenced OFs directly, forecasting models have the possibility of combining order flows from bid and ask sides asymmetrically.

**2.2. Forecasting Models.** In this section we describe the ANNs we use in our study. In particular, we consider an MLP, single and stacked LSTM, LSTM-MLP,

and CNN-LSTM. Besides the CNN-LSTM that is similar in spirit to the architecture used by Zhang et al. (2018), all other models are standard “off-the-shelf” ANNs and we keep their descriptions brief. For an introduction to DL and a discussion of many of the standard ANN architectures, we refer to Goodfellow et al. (2016) and Friedman et al. (2017). For comparative purposes, we also include a classical linear ARX model in our empirical work.

**2.2.1. ARX.** An *autoregressive with exogenous inputs* (ARX) model, based on a traditional autoregressive (AR) model (Hamilton, 1994), is a time series model where the dependent variable,  $y_t \in \mathbb{R}$ , is regressed onto lagged versions of itself and vectors of exogenous inputs,  $\mathbf{x}_t \in \mathbb{R}^m$ , that is

$$y_t = w_0 + \sum_{i=1}^{n_y} w_i y_{t-i} + \sum_{i=1}^{n_x} \mathbf{v}_i^\top \mathbf{x}_{t-i} + \varepsilon_t, \quad (6)$$

where  $w_0, w_i \in \mathbb{R}$  and  $\mathbf{v}_i \in \mathbb{R}^m$  are parameters,  $\varepsilon_t$  is a random white noise term with zero mean, and  $n_y, n_x$  denote the orders of the autoregressive and exogenous inputs, respectively. We refer to (6) as an  $\text{ARX}(n_y, n_x)$  model.

In our empirical work, we explored two formulations using 100 lags. In the first one, we regressed mid-price returns on lagged versions of itself and OFs for the top ten levels of the LOB. In the second, we regressed mid-price returns only on lagged OFs up to ten levels. Effectively, the second formulation is a standard linear regression of the forward returns on (lagged) OFs. We found the results from these two formulations to be similar. Therefore, in the empirical section of this article we only report the results for the latter.

**2.2.2. Multilayer Perceptron.** A *multilayer perceptron* (MLP) is a *feedforward artificial neural network* (FFNN) that consists of  $L \geq 1$  hidden layers, each with  $N_l \in \mathbb{N}$  neurons. Given an input vector  $\mathbf{x} \equiv \mathbf{h}_0 \in \mathbb{R}^{N_0}$ , an MLP with  $L$  hidden layers is a mapping of the form

$$\mathbf{h}^{(l)} = g^{(l)}(\mathbf{W}^{(l)} \mathbf{h}^{(l-1)} + \mathbf{b}^{(l)}), \quad l = 1, 2, \dots, L, \quad (7)$$

$$\mathbf{y} = \mathbf{W}^{(L+1)} \mathbf{h}^{(L)} + \mathbf{b}^{(L+1)}, \quad (8)$$

where  $\mathbf{h}^{(l)} \in \mathbb{R}^{N_l}$  is the hidden state of the  $l$ -th layer,  $\mathbf{W}^{(l)} \in \mathbb{R}^{N_l \times N_{l-1}}$  is a weight matrix,  $\mathbf{b}^{(l)} \in \mathbb{R}^{N_l}$  is a bias vector, and  $\mathbf{y} \in \mathbb{R}^{N_{L+1}}$  is the output. Here,  $g^{(l)} : \mathbb{R} \rightarrow \mathbb{R}$  is an activation function that acts component-wise on its argument. In this article we use the *rectified linear unit* (ReLU) activation function, i.e.  $g^{(l)}(x) := \max(0, x)$  for all  $l$ .

We emphasize that while an MLP is a universal approximator (Hornik, 1991), it is not inherently designed to model time dependencies as it lacks spatiotemporal invariance. In particular, as each timestamp is treated independently by an MLP,



the temporal information is lost. In addition, the number of parameters in each layer of an MLP is not invariant across time series of different lengths, making transferability of the network challenging (Fawaz et al., 2019).<sup>3</sup> In the horse race conducted by Briola et al. (2020) they compare classical ML approaches and DL in forecasting high-frequency returns from LOB data using classification. Their results suggest, as a universal function approximator, a large enough MLP performs as well as the CNN-LSTM of Zhang et al. (2018).

**2.2.3. Long Short-Term Memory and Extensions.** First introduced by Hochreiter et al. (1997) *long short-term memory* (LSTM) is an ANN explicitly designed to handle temporal dependencies in sequential data. Belonging to the family of *recurrent neural networks* (RNNs), LSTMs address the vanishing gradient problem that is common in training traditional RNNs (Rumelhart et al., 1986). The key elements of the LSTM are (i) a memory cell, representing its state over time, that is combined with (ii) non-linear gates that determine the information flow in and out of the memory cell. Commonly, three gates are used, referred to as input, output, and forget gates (Gers et al., 2000). Letting  $\mathbf{x}_t \in \mathbb{R}^N$  denote an input vector, the LSTM unit takes the form<sup>4</sup>

$$\mathbf{f}_t = \sigma(\mathbf{U}^f \mathbf{x}_t + \mathbf{W}^f \mathbf{h}_{t-1} + \mathbf{b}^f) \quad (9)$$

$$\mathbf{i}_t = \sigma(\mathbf{U}^i \mathbf{x}_t + \mathbf{W}^i \mathbf{h}_{t-1} + \mathbf{b}^i) \quad (10)$$

$$\mathbf{o}_t = \sigma(\mathbf{U}^o \mathbf{x}_t + \mathbf{W}^o \mathbf{h}_{t-1} + \mathbf{b}^o) \quad (11)$$

$$\mathbf{s}_t = \mathbf{f}_t \circ \mathbf{s}_{t-1} + \mathbf{i}_t \circ \tanh(\mathbf{U}^s \mathbf{x}_t + \mathbf{W}^s \mathbf{h}_{t-1} + \mathbf{b}^s) \quad (12)$$

$$\mathbf{h}_t = \mathbf{o}_t \circ \tanh(\mathbf{s}_t) \quad (13)$$

where  $\sigma := (1 + e^{-x})^{-1}$  is the sigmoid activation function,  $\mathbf{f}_t \in \mathbb{R}^M$  is the forget gate's activation vector,  $\mathbf{i}_t \in \mathbb{R}^M$  is the input gate's activation vector,  $\mathbf{o}_t \in \mathbb{R}^M$  is the output gate's activation vector,  $\mathbf{h}_t \in \mathbb{R}^M$  is the output vector of the LSTM unit,  $\mathbf{s}_t \in \mathbb{R}^M$  is the unit's hidden state vector, and  $\mathbf{W} \in \mathbb{R}^{M \times N}$ ,  $\mathbf{U} \in \mathbb{R}^{M \times M}$  and  $\mathbf{b} \in \mathbb{R}^M$  (superscripts dropped) are weight matrices and bias vector parameters that are learned during training. Here,  $\circ$  and  $\tanh$  denote the element-wise product and hyperbolic tangent, respectively. To avoid the vanishing gradient problem, we initialize  $\mathbf{b}^f$  to one when training our networks (Gers et al., 2000).

<sup>3</sup>Transfer learning is the ability to reuse a pre-trained neural network on a new problem. Besides the compute and time savings transfer learning provides, it is particularly useful in many financial application as many real-world problems do not have large enough training datasets to train models from scratch (Pan et al., 2009; Bengio, 2012).

<sup>4</sup>This formulation follows Keras' default implementation of the LSTM, available at [https://www.tensorflow.org/api\\_docs/python/tf/keras/layers/LSTM](https://www.tensorflow.org/api_docs/python/tf/keras/layers/LSTM), which is what we use in our empirical work.

In applications, the output from an LSTM frequently feeds into an MLP, referred to as an *LSTM-MLP* architecture. In this model setup, temporal dependencies in the input are preserved by an LSTM, and the extracted embedding (i.e. the transformed input) is then passed to an MLP.

By combining multiple LSTMs in such a way that the output of one LSTM becomes the input to another LSTM, we obtain a *stacked LSTM* architecture, a deeper version of the LSTM (Graves, 2013; Graves et al., 2013). A generic stacked LSTM consists of several hidden LSTM layers each containing multiple memory cells. Each layer provides a sequential output rather than a single value to the next layer, allowing the hidden state at each level to operate at different timescales.

In a large-scale comparison of eight shallow LSTM variants, Greff et al. (2016) demonstrate they perform well on a range of tasks, including speech and handwriting recognition, and polyphonic music modeling. Pascanu et al. (2013) confirm that deeper architectures outperform conventional shallow networks in polyphonic music prediction and language modeling tasks. Recent work by Sirignano (2019) and Tsantekidis et al. (2020) provide support for LSTMs being able to forecast high-frequency returns using order book data.

**2.2.4. CNN-LSTM.** While standard ANNs such as CNNs<sup>5</sup>, LSTMs, and MLPs can be used individually, it is well-known they are complementary in their modeling capabilities and therefore each can be found as building blocks in combined network architectures. For instance, CNNs are effective in reducing frequency variations, LSTMs excel in learning temporal structures, and MLPs are universal approximators. Therefore, used together in combined networks, each extracts information from the input at different spatial and temporal scales (Sermanet et al., 2011; Sainath et al., 2015). Notably, the work of Sainath et al. (2015) is one of the first to combine CNNs, LSTMs, and MLPs into a unified architecture that can be trained jointly. CNN-LSTMs have been used successfully in a number of applications, including image and video recognition (Donahue et al., 2015; Vinyals et al., 2015), language modeling (Kim et al., 2016) and nowcasting (Shi et al., 2015).

The CNN-LSTM we employ in this article is similar in spirit to the architecture used by Zhang et al. (2018). While they forecast high-frequency returns as a classification task, we use the multi-horizon regression framework described in Section 3.2.<sup>6</sup> Because the CNN-LSTM for LOB inputs is the most general, we describe it first and later comment on how we modify it for OF inputs. The specific details

<sup>5</sup>*Convolutional neural networks* (CNNs) are multilayer FFNNs first popularized in image processing, obtaining their name from having layers consisting of convolutional filters. CNNs are translation equivariant and can be viewed as regularized versions of MLPs. See, Goodfellow et al. (2016) for an introduction to CNNs.

<sup>6</sup>The implementation of Zhang et al. (2018) is available at <https://github.com/zcakhha/DeepLOB-Deep-Convolutional-Neural-Networks-for-Limit-Order-Books>.

| Block    | Description   | Details  | Layer Input                       | Layer Output              |
|----------|---|--|-----------------------------------|---------------------------|
| <b>1</b> | <b>Convolutions of prices and volumes</b>   |  |                                   |                           |
|          | (i) Combine price and volume information for each side and level of the order book                          | One spatial convolution ( $1 \times 2$ ) (stride = $1 \times 2$ ) with 32 filters  | $100 \times 40 \times 1$          | $100 \times 20 \times 32$ |
|          | (ii) Combine price-volume information across time for each side and level of the order book                 | Two temporal convolutions ( $4 \times 1$ ) (stride = $1 \times 1$ ) with 32 filters and padding  | $100 \times 20 \times 32$         | $100 \times 20 \times 32$ |
| <b>2</b> | <b>Convolutions across LOB levels<sup>a</sup></b>   |  |                                   |                           |
|          | (i) Combine imbalance information across sides for each level of the order book                             | One spatial convolution ( $1 \times 2$ ) (stride = $1 \times 2$ ) with 32 filters  | $100 \times 20 \times 32^b$       | $100 \times 10 \times 32$ |
|          | (ii) Combine imbalance information across time for each side and level of the order book                    | Two temporal convolutions ( $4 \times 1$ ) (stride = $1 \times 1$ ) with 32 filters and padding  | $100 \times 10 \times 32$         | $100 \times 10 \times 32$ |
| <b>3</b> | <b>Convolutions of imbalance information</b><br>Combine imbalance information across all levels of the book | One spatial convolution ( $10 \times 1$ ) (stride = $1 \times 10$ ) with 32 filters  | $100 \times 10 \times 32^c$       | $100 \times 1 \times 32$  |
| <b>4</b> | <b>Inception module</b>   | The inception module consists of 3 subblocks, each acting on the output from block 3 above. Each sub-block uses 64 filters. Outputs are then concatenated and reshaped before being passed to the LSTM |                                   |                           |
|          | Subblock 1  | Spatial convolution ( $1 \times 1$ ) and temporal convolution ( $3 \times 1$ ) (stride = $1 \times 1$ ) with 64 filters and padding  | $100 \times 1 \times 32$          | $100 \times 1 \times 64$  |
|          | Subblock 2  | Spatial convolution ( $1 \times 1$ ) and temporal convolution ( $5 \times 1$ ) (stride = $1 \times 1$ ) with 64 filters and padding  | $100 \times 1 \times 32$          | $100 \times 1 \times 64$  |
|          | Subblock 3  | Spatial max pooling and temporal convolution ( $1 \times 1$ ) (stride = $1 \times 1$ ) with 64 filters and padding   | $100 \times 1 \times 32$          | $100 \times 1 \times 64$  |
|          | Concatenation and reshaping   |  | $100 \times 1 \times 64 \times 3$ | $100 \times 192$          |
| <b>5</b> | <b>LSTM</b><br>The output of the LSTM is an alpha term structure  | LSTM with 64 hidden units  | $100 \times 192$                  | $10 \times 1$             |

TABLE 1. The CNN-LSTM architecture for LOB inputs. The architectures for OF inputs involve just block 2 through block 5.

<sup>a</sup>For LOB inputs these are convolutions of notional features (in dollars), while for OF inputs these are convolutions of volumes (number of shares).<sup>b</sup>This is the size for LOB inputs. For OF inputs the size is  $100 \times 20 \times 1$ .<sup>c</sup>This is the size for LOB and OF inputs. For OFI inputs the size is  $100 \times 10 \times 1$ .

of the architecture, including descriptions of each layer, is elucidated in Table 1. To keep this table and following description concise, we assume the reader is familiar with convolutions and CNNs as described in the textbook by Goodfellow et al. (2016).

From a high-level perspective, the architecture consists of (i) a CNN, (ii) an inception module, and (iii) an LSTM, each consisting of one or more blocks and subblocks (see the first two columns of Table 1). The CNN is made up of three blocks. Block 1 reduces the spatial dimension of the input from 40 to 20 by combining prices and volumes. Block 2 further reduces the spatial dimension from 20 to 10 by combining information across bid and ask sides at the same level of the order book. Then, by aggregating information across all levels in the order book, block 3 reduces the spatial dimension down to one. All activation functions in the CNN blocks are *leaky ReLUs*, i.e.  $g(x) := \max(0, x) + 0.01 \min(0, x)$ . The inception module is a standard architectural element in CNNs used for extracting features at different temporal frequencies (Szegedy et al., 2015). Finally, after concatenating and reshaping the outputs of the inception module, an LSTM with 64 hidden units is used to extract temporal features, returning an alpha term structure.

The different sizes of the OF inputs necessitate small adjustments of the CNN-LSTM architecture. In particular, for OF inputs it consists of block 2 through block 5 in Table 1, where the input to the first layer is of size  $100 \times 20 \times 1$ . Otherwise, the CNN-LSTM architectures for OF inputs are the same as the one with LOB inputs.

### 3. DATA AND METHODOLOGY

**3.1. Data.** We source our data from LOBSTER (Huang et al., 2011). This dataset provides complete order book state information from Nasdaq, except for submissions and cancellations of hidden orders. We include all stocks from January 1, 2019 through January 31, 2020 that meet the following three criteria: (i) their being a member of the Nasdaq 100 index at some point during the time period, (ii) their having data for at least 260 trading days, and (iii) their having no corporate actions during the period of study. Due to issues with the underlying data, January 9, 2019 is excluded. This results in a universe of 115 stocks, containing many household names across a variety of industries, including Amazon (AMZN), American Airlines (AAL), Facebook (FB), Google (GOOGL), Microsoft (MSFT), and Netflix (NFLX). The larger number of stocks and longer time period than most previous studies provide greater reliability in results from our out-of-sample testing and allow us to explore stock specific properties.

LOBSTER data must be preprocessed before use (Bouchaud et al., 2018; Bugaenko, 2020). The preprocessing addresses situations such as that of a single market order executing against multiple limit orders, or a modification to a limit order being

implemented as a cancellation followed by a new submission. We describe our preprocessing steps in Appendix A.

Our preprocessed dataset, summarized in Table 6 in Appendix A, is identical to that used in Kolm et al. (2021) with a size of about 10TB uncompressed. As a result, storage and efficient processing become challenging tasks. Our dataset is one to two orders of magnitude larger than similar studies that apply deep learning to limit order books (Tsantekidis et al., 2017; Tran et al., 2019; Zhang et al., 2018; Zhang et al., 2019a; Zhang et al., 2019b; Tsantekidis et al., 2020; Briola et al., 2020; Zhang et al., 2021a; Zhang et al., 2021b)). The datasets used by Sirignano (2019) and Sirignano et al. (2019) are exceptions. Their universe is drawn from the S&P 500 and is larger than ours; however, their focus is on a single architecture. Sirignano (2019) uses a spatial neural network architecture and Sirignano et al. (2019) focuses on a stacked LSTM, both in a classification setting. In contrast we consider MLP, LSTM, LSTM-MLP, stacked LSTM and CNN-LSTM architectures in a multi-horizon regression setting, allowing us to compare and shed light on which aspects of the architectures are most useful for predicting high-frequency returns while still ensuring the results apply to a broad universe of stocks.

**3.2. Methodology.** We focus on simultaneously forecasting future mid-price returns across multiple horizons. In particular, for each stock and time  $t$ , our multi-horizon forecasts are represented as the vector

$$\mathbf{r}_t := (r_{t,1}, \dots, r_{t,H})^\top \in \mathbb{R}^H, \text{ where } H \geq 1, \quad (14)$$

where  $H$  denotes the number of horizons. We refer to (14) as an *alpha term structure* at time  $t$ . Our forecasting models are trained at the single stock level and take the form

$$\mathbf{r}_t = \mathbf{g}(\mathbf{x}_t, \mathbf{x}_{t-1}, \dots, \mathbf{x}_{t-W}) + \varepsilon_t, \quad (15)$$

where the vector-valued function  $\mathbf{g}$  is approximated by an ANN,  $\varepsilon_t \in \mathbb{R}^H$  is the residual,  $W$  denotes the length of the lookback window, and the input,  $\{\mathbf{x}_\tau\}_{\tau=t}^{t-W}$ , is either LOBs or OFs at the most granular tick level. As is common in the literature, in our empirical work we set  $W = 100$  for all symbols, (see, for example, Zhang et al. (2019a)). The robustness check we perform in Appendix B.2, using stock specific lookback windows, suggests that window length is less important as a driver of predictive performance. To avoid issues around market open and close, we drop the first and last ten minutes of each day in our empirical work.

A question investigated in Sirignano et al. (2019) is whether the function  $\mathbf{g}$  in (15) is *universal*, i.e. if the same function is *shared across stocks*. To estimate their model Sirignano et al. (2019) downsample the time series of updates to the order book to only those times where price changes occur. It is well-known in the

market microstructure literature that not just trades but all changes to the order book are important in understanding price formation (see, for example, Cont et al. (2014) and Bouchaud et al. (2018)). Therefore, as our focus in this article is return forecasting rather than questions of universality, and downsampling risks removing potentially important information, we use all order book updates and train an ANN for each symbol in the dataset.

**3.2.1. Dependent Variables.** Our stock universe contains a diverse set of symbols with significantly different order book activity. For instance, EBAY and MSFT differ by three orders of magnitude in terms of number of order book updates per day (see, Table 6 in Appendix A). The wide-ranging update frequencies are related to the notion of what the practitioner community refers to as “stock characteristic time” and can be formalized by intermittent processes such as Hawkes processes (see, for example, Jaisson et al. (2016) and Bouchaud et al. (2018)). Using single stock models in our work, we make the horizons of the alpha term structure in equation (14) stock specific. Specifically, we define a stock specific time increment

$$\Delta t := \frac{2.34 \cdot 10^7}{N}, \quad (16)$$

where the numerator is the number of milliseconds in a trading day, and the denominator,  $N$ , denotes the average number of non-zero tick-by-tick mid-price returns. This ratio measures how long on average we have to wait for a non-zero mid-price return for a given stock.

We choose an alpha term structure (14) of dimension  $H = 10$  and define our forecast horizons,  $\{h_k\}_{k=1}^{10}$ , as the following multiples of  $\Delta t$

$$h_k := \frac{1}{5}k\Delta t, k = 1, \dots, 10. \quad (17)$$

As dependent variables in our single stock forecasting models (15) we use the  $h_k$ -horizon mid-price returns  $r_{t,k} := p_{t+h_k} - p_{t+\delta\tau}$  (in dollars), where  $p_t$  denotes the mid-price at time  $t$  and  $\delta\tau$  represents a ten millisecond latency buffer. Analogously, we evaluate model performance by computing out-of-sample returns in the same way. It is common practice to use latency buffers in developing and testing alphas to account for delays associated with the time needed to compute model forecasts and the round-trip communication time between the exchange and the trading algorithm. Using Nasdaq-sourced data for one month in 2007 and 2008, respectively, Hasbrouck et al. (2013) estimate the fastest traders in their sample had an effective latency of 2–3 milliseconds. Zhang et al. (2019a) report that the average time needed to produce a return forecast from a number of state-of-the-art ANNs, including that of a CNN and LSTM, ranges from 0.03 to 0.97 milliseconds,

depending on the model used. Hence, the ten millisecond latency buffer we use in this study is conservative.

Using stock specific forecast horizons ensures the time scale adjusts appropriately for each stock. Naturally, due to non-constant volume and volatility profiles throughout a typical trading day, the average time for a price change is not uniform. Therefore, the specification of the forecast horizons can certainly be improved to take various intraday and trading related effects into account. Needless to say, the ones we use here are parsimonious and allow us to sensibly compare results across stocks in our empirical analysis. While generalizations that incorporate intraday profiles are possible within our framework (see, for example, Mertens et al., 2019), we leave this for future work.

*3.2.2. Independent Variables.* We consider two choices of independent variables as inputs to our models, LOBs and OFs, defined in equations (1) and (4), respectively. LOBs provide a complete representation of the order book. In general, while return series are stationary, price series tend to be nonstationary (Cont, 2001). Therefore, we expect order book states to be nonstationary, and the resulting regression problem in (15) will have stationary dependent variables and nonstationary independent variables. In contrast, as emphasized in Section 2.1.2, OFs are reduced stationary representations of order book states. Unlike OFIs (defined in equation (5)), OFs keep bid and ask sides separate, thereby enabling models to incorporate them asymmetrically.

We winsorize all dependent and independent variables in our training sets at the 0.5% and 99.5% levels and then perform  $Z$ -score normalization of the resulting data. The parameters from the in-sample normalization are stored to scale test and validation sets that are used for out-of-sample evaluation.

*3.2.3. Training and Evaluation.* Our training and evaluation procedure is similar to a real-world production setting. In particular, we train our models in a rolling-window backtesting fashion across 48 weeks using a (1 week, 4 weeks, 1 week) structure, where the first week is used for validation, the following four weeks are used for training, and the last week is reserved for out-of-sample testing. To keep the training data for consecutive windows non-overlapping we move our rolling window forward by three weeks each time. With 115 symbols, 12 model and input combinations, and 18 rolling windows, we train and evaluate a total of about 25K individual model fits. To the best of our knowledge, previous studies in this area do not perform out-of-sample testing on a rolling basis. While rolling comes at a significantly higher computational cost as many models need to be trained and retrained, empirical findings will be more reliable as out-of-sample forecasting performance can be evaluated over longer time periods.

| Model    | Input | Number of layers | Number of parameters <sup>(*)</sup> | Learning rate | Batch size | Training epochs | Early stopping |
|----------|-------|------------------|-------------------------------------|---------------|------------|-----------------|----------------|
| ARX      | OF    | 1                | $2.0 \times 10^3$                   | $10^{-4}$     | 256        | 50              | Yes            |
| CNN-LSTM | OF    | 27               | $1.3 \times 10^5$                   | $10^{-3}$     | 256        | 50              | Yes            |
| LSTM     | OF    | 2                | $1.0 \times 10^5$                   | $10^{-5}$     | 256        | 50              | Yes            |
| LSTM (3) | OF    | 4                | $4.6 \times 10^5$                   | $10^{-5}$     | 256        | 50              | Yes            |
| LSTM-MLP | OF    | 3                | $8.4 \times 10^4$                   | $10^{-5}$     | 256        | 50              | Yes            |
| MLP      | OF    | 4                | $1.3 \times 10^6$                   | $10^{-5}$     | 256        | 50              | Yes            |
| ARX      | LOB   | 1                | $4.0 \times 10^3$                   | $10^{-4}$     | 256        | 50              | Yes            |
| CNN-LSTM | LOB   | 27               | $1.4 \times 10^5$                   | $10^{-3}$     | 256        | 50              | Yes            |
| LSTM     | LOB   | 2                | $1.1 \times 10^5$                   | $10^{-5}$     | 256        | 50              | Yes            |
| LSTM (3) | LOB   | 4                | $4.7 \times 10^5$                   | $10^{-5}$     | 256        | 50              | Yes            |
| LSTM-MLP | LOB   | 3                | $9.4 \times 10^4$                   | $10^{-5}$     | 256        | 50              | Yes            |
| MLP      | LOB   | 4                | $2.3 \times 10^6$                   | $10^{-5}$     | 256        | 50              | Yes            |

TABLE 2. Summary of inputs and hyperparameters for the models in this article.  
<sup>(\*)</sup>The number of parameters are approximated to the nearest order of magnitude and truncated for readability.

We train our models by minimizing mean-squared error (MSE) with *stochastic gradient descent* (SGD) using the Adam optimizer (Kingma et al., 2014). Table 2 summarizes all input and hyperparameter settings. The batch size is kept small as there is evidence that smaller batch sizes lead to local minima which generalize better (Keskar et al., 2017). If the time series of order book updates and returns are naively concatenated, elements in a batch can contain data from two separate trading days. To avoid this we implement a custom Keras generator. We apply early stopping for all models to avoid overfitting, terminating training when validation loss has not decreased for five consecutive epochs. Our code is written in Python and ANNs are implemented with Tensorflow 2.3.1 (Abadi et al., 2015) and Keras (Chollet et al., 2015).

Simple models like MLP/ARX can be trained directly using CPUs. However, training DL models incorporating CNNs and LSTMs would most likely be impossible without the use of GPUs. When fitting our LSTM and CNN-LSTM-based models, we use single GPUs, which are either an NVIDIA Quadro RTX8000 (48GB), an NVIDIA V100 (32GB), or an AMD MI-50 (32GB). All of our computations are performed on NYU’s Greene<sup>7</sup> and Hudson<sup>8</sup> high performance computing environments. This infrastructure allows us to massively parallelize the data processing and training of the models. The time to train a single model varies in the range of 10-60 minutes, depending on model and stock.

<sup>7</sup>Greene has 32K CPU cores, 332 NVIDIA GPUs and 145TB of RAM distributed over 568 nodes. See, <https://www.nyu.edu/about/news-publications/news/2020/november/GreeneSupercomputer.html>.

<sup>8</sup>Hudson has 960 CPU cores, 160 AMD GPUs and 10TB of RAM distributed across 20 nodes. See, <https://wp.nyu.edu/connect/2020/06/08/nyu-expands-supercomputing-amd>.



We evaluate the performance of each forecasting model at the individual stock level using *out-of-sample*  $R^2$  at horizon  $h$  ( $R_{OS,h}^2$ ) for each test period, defined as

$$R_{OS,h}^2 := 1 - \text{MSE}_{m,h} / \text{MSE}_{\text{bmk},h}, \quad (18)$$

where  $\text{MSE}_{m,h}$  and  $\text{MSE}_{\text{bmk},h}$  are the mean-squared errors of the model forecasts and benchmark at the  $h$ -th horizon, respectively. To be conservative, we use the average out-of-sample return as our benchmark. If  $R_{OS,h}^2 > 0$ , then the forecasting model outperforms the benchmark represented by the average return on the test set. Importantly, a forecast relies only on data available up to the time at which it is computed. When it is clear what the horizon is, in the remainder of the article we sometimes drop the subscript  $h$  and just write  $R_{OS}^2$ .

To statistically examine questions such as the relative forecast accuracy of model and input combinations, what kind of input works better for particular models, and whether particular models exhibit superior forecasting ability, we use the standard methodology of Patton (2011) and Liu et al. (2015).

#### 4. EMPIRICAL RESULTS

In this section we present our empirical results divided into three parts. First, in Section 4.1 we investigate short-term return predictability (less than two average price changes) at the individual stock level. We evaluate which model and input combination deliver the best performance and examine statistically the question of whether there is superior forecasting ability at short horizons. Using cross-sectional regressions, in Section 4.2 we link the forecasting performance of the LSTM trained on OF inputs to stock characteristics at the market microstructure level. Finally, in Section 4.3, we analyze return predictability of the CNN-LSTM, LSTM, and LSTM-MLP, all trained on OF inputs, on longer time scales (up to ten average price changes). In our empirical work,  $t$ - and  $F$ -statistics are calculated using heteroskedasticity-consistent standard errors (White, 1980).

**4.1. Short-Term Return Predictability.** Figure 2 presents the out-of-sample forecasting performance of the models at different horizons using OF inputs (left panel) and LOB inputs (right panel). We train each model using the rolling-window out-of-sample methodology across 48 weeks as described in Section 3.2.3, measuring performance as the average  $R_{OS}^2$  across days and stocks. To produce the curve for each model, we first compute the daily average  $R_{OS}^2$  for each stock and horizon. The resulting performance across stocks is then averaged to obtain the average  $R_{OS}^2$  for each model. Recall that horizons are determined as the fraction of an average price change for each stock (see Section 3.2.1).

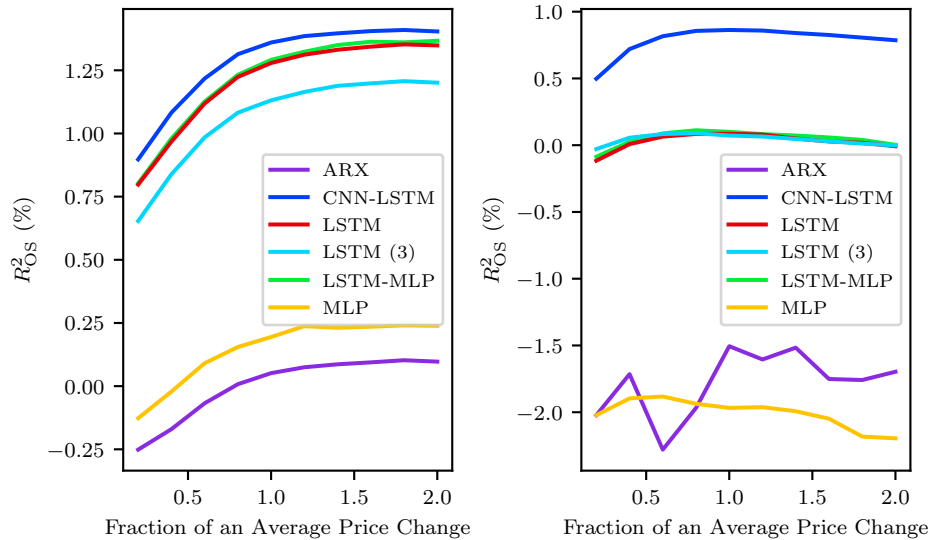


FIGURE 2. Out-of-sample forecasting performance of the models at different horizons from 10 levels of order flows (left panel) and order book states (right panel). Model performance is measured as the average  $R^2_{OS}$  across days and stocks. Horizons are given as the fraction of an average price change for each stock. Each model is trained using a rolling-window out-of-sample methodology across 11 months of data.

Except for the CNN-LSTM, it is apparent that the models are not able to learn from LOBs.<sup>9</sup> As OFs represent a particular transformation of the LOBs, given enough data ANNs trained on LOBs should in principle be able to learn this (or perhaps an even better) transformation. This was the main motivation for the CNN-LSTM architecture of Zhang et al. (2019b). However, comparing the left and right panels in Figure 2, OFs deliver better predictive performance for all models considered, independent of model structure or complexity.

The left panel of Figure 2 suggests that the predictive power as measured by average  $R^2_{OS}$  increases up to two average price changes for most models. This is in line with expectations. As our models are trained on data at the highest frequency with a relatively short lookback window, we do not expect to generate alphas with a long horizon. In Section 4.3, we examine return predictability beyond two average price changes of the CNN-LSTM, LSTM, LSTM-MLP trained on OF inputs.

The left panel of Figure 2 also shows that ANNs with at least one LSTM module perform significantly better than the ARX and MLP models. In the case of the MLP, a standard explanation for its underperformance would be that, despite early stopping, the large number of parameters leads to overfitting the training data

<sup>9</sup>Of course, an ARX is not sensible in the case of LOBs as the regressors are nonstationary. We include it for completeness only.

and results in poor generalization. More recently though, Wilson et al. (2020) emphasize that “parameter counting is a poor proxy for understanding generalization behaviour.” The authors highlight the notion of the *inductive biases* of a model, which in a Bayesian framework describes the datasets that are likely under the model in question. While our approach is not Bayesian, we believe this reasoning applies here. Specifically, as order book data has a natural ordering, we expect the underlying data generating process to exhibit temporal dependence. An LSTM is intrinsically a sequential model which naturally captures the temporal dependence, thereby leading to better generalization than an MLP.

*4.1.1. Rankings of Average Forecast Accuracy.* Training the six models on either LOB or OF inputs results in twelve model and input combinations. To compare their out-of-sample performance, we rank them by their average forecast accuracy as follows. For each day, stock, and horizon, we rank the combinations from best to worst based on their  $R_{OS}^2$ , such that the best combination receives a rank of 1 and the worst receives a rank 12. Then for each day, we average the ranks for each combination across stocks, arriving at a daily average rank for each model, input, and horizon. Then, by averaging the daily average ranks over the whole test set we obtain a global average rank for each model, input, and horizon. These ranks are displayed in the first ten columns of Figure 3. Similarly, by first averaging the daily average ranks of all the horizons and then averaging over the whole test set, we obtain a global average rank for all models, denoted by “Avg” in Figure 3.

There are two key practical take-aways from the figure. First, ANN models with OF input consistently outperform their LOB counterparts. Second, once an ANN has an LSTM as part of its architecture, its predictive performance increases significantly over the ARX and MLP models we use in this article.

*4.1.2. Should One Use Order Flow or Limit Order Book Inputs?* To assess whether OF or LOB inputs are better, we follow Patton (2011) and Liu et al. (2015), performing pairwise comparisons of each model where the only difference is the input they have been trained on. The comparisons are done as follows. For each model, forecast horizon, and stock, we first compute the  $t$ -statistic of the average difference in  $R_{OS}^2$  that result from using OF and LOB inputs. Then for each horizon, we calculate the difference between the number of stocks with a significantly positive and negative  $t$ -statistics at a significance level of 1%. The results are displayed in the first ten columns of Table 3. Here, a positive difference of  $X$  implies that the model with OF inputs outperforms the same model with LOB inputs for  $X$  stocks in our sample. We repeat the same analysis after first averaging  $R_{OS}^2$  across the alpha term structure for each model, stock, and day. Then as before, we calculate

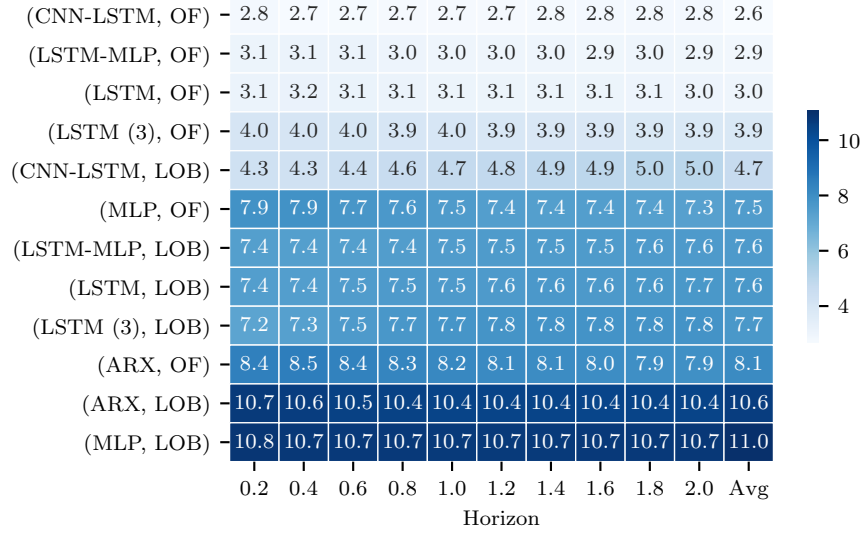


FIGURE 3. Average ranks of model and input combinations by horizon. The best performing combination for each symbol and day receives a rank of 1, and the worst receives a ranks 12. The last column, denoted by “Avg,” displays rankings based first averaging the daily average ranks of all horizons and then averaging over the whole test set to obtain a global average rank for all models. It is apparent that ANN models with OF input consistently outperform their LOB counterparts.

the difference between the number of stocks with a significantly positive and negative  $t$ -statistics at a significance level of 1%, presenting these results in the column denoted by “Avg” in Table 3.

We observe that all models with OF inputs outperform the same models with LOB inputs. This result is particularly strong for the LSTM, LSTM (3) and LSTM-MLP models, where for almost all horizons, OF inputs outperform across the 115 stocks. Interestingly, at the shorter forecasting horizons, there are about 40 stocks for which the CNN-LSTM with LOB inputs perform better, whereas beyond one average price change OF inputs dominate.

**4.1.3. Is There Superior Forecasting Ability?** Above we demonstrated that the best performing model and input combinations are: (i) ANNs with at least one LSTM module trained on OFs inputs, and (ii) the CNN-LSTM trained on LOBs. Next, following Patton (2011) and Liu et al. (2015), we test whether these models have an  $R_{OS}^2$  that is significantly greater than 0. We perform these tests as follows. For each model, forecasting horizon and stock, we first compute a  $t$ -statistic of their average  $R_{OS}^2$ . Then for each horizon, we calculate the difference between the number of significantly positive and negative  $t$ -statistics (at a significance level of 1%). The results are displayed in the first ten columns of Table 4, where a positive entry

| Model    | Horizon (Fraction of Avg Price Change) |     |     |     |     |     |     |     |     |     | Avg |
|----------|--|-----|-----|-----|-----|-----|-----|-----|-----|-----|-----|
|          | 0.2                                    | 0.4 | 0.6 | 0.8 | 1.0 | 1.2 | 1.4 | 1.6 | 1.8 | 2.0 |     |
| LSTM     | 115                                    | 115 | 115 | 115 | 115 | 114 | 115 | 115 | 115 | 115 | 115 |
| LSTM (3) | 114                                    | 115 | 115 | 115 | 115 | 115 | 115 | 114 | 115 | 114 | 115 |
| LSTM-MLP | 115                                    | 115 | 114 | 114 | 115 | 114 | 115 | 115 | 114 | 115 | 115 |
| MLP      | 111                                    | 110 | 109 | 110 | 111 | 110 | 110 | 110 | 110 | 110 | 110 |
| ARX      | 101                                    | 94  | 89  | 90  | 91  | 90  | 92  | 91  | 93  | 94  | 93  |
| CNN-LSTM | 70                                     | 76  | 81  | 86  | 89  | 91  | 92  | 91  | 93  | 92  | 89  |

TABLE 3. Summary results of pairwise comparisons of the  $R_{OS}^2$  from models using either LOB or OF inputs. For each model, forecasting horizon and stock, we first compute a  $t$ -statistic of the average loss difference that result from using OF and LOB inputs. We obtain each table entry by calculating the difference between the number of significantly positive and negative  $t$ -statistics (at a significance level of 1%). To produce the rightmost column, at each point in time we first average the  $R_{OS}^2$  across the alpha term structure. Then we calculate the difference between the number of significantly positive and negative  $t$ -statistics (at a significance level of 1%). A positive entry  $X$  implies that the model with OF inputs outperformed the same model with LOB inputs for  $X$  stocks in our sample.  $t$ -statistics are calculated using heteroskedasticity-consistent standard errors (White, 1980).

| Model           | Horizon (Fraction of Avg Price Change) |     |     |     |     |     |     |     |     |     | Avg |
|-----------------|--|-----|-----|-----|-----|-----|-----|-----|-----|-----|-----|
|                 | 0.2                                    | 0.4 | 0.6 | 0.8 | 1.0 | 1.2 | 1.4 | 1.6 | 1.8 | 2.0 |     |
| (CNN-LSTM, OF)  | 97                                     | 103 | 109 | 109 | 109 | 108 | 109 | 109 | 109 | 108 | 110 |
| (LSTM, OF)      | 90                                     | 98  | 103 | 105 | 109 | 108 | 108 | 107 | 107 | 109 | 109 |
| (LSTM-MLP, OF)  | 93                                     | 96  | 105 | 108 | 110 | 110 | 108 | 107 | 107 | 107 | 109 |
| (LSTM (3), OF)  | 75                                     | 89  | 98  | 101 | 106 | 106 | 105 | 106 | 106 | 105 | 107 |
| (CNN-LSTM, LOB) | 47                                     | 61  | 66  | 68  | 73  | 72  | 74  | 73  | 74  | 74  | 69  |

TABLE 4. Summary of the number of models trained on LOB and OF inputs that have an  $R_{OS}^2$  that is significantly greater than 0. For each model, forecasting horizon and stock, we first compute a  $t$ -statistic of the average  $R_{OS}^2$ . We obtain each table entry by calculating the difference between the number of significantly positive and negative  $t$ -statistics (at a significance level of 1%). To produce the rightmost column, at each point in time we first average the  $R_{OS}^2$  across the alpha term structure. Then we calculate the difference between the number of significantly positive and negative  $t$ -statistics (at a significance level of 1%). A positive entry  $X$  implies that the model has an  $R_{OS}^2$  that is significantly greater than 0 for  $X$  stocks in our sample.  $t$ -statistics are calculated using heteroskedasticity-consistent standard errors (White, 1980).

$X$  implies that the model has an  $R_{OS}^2$  that is significantly greater than 0 for  $X$  stocks in our sample. We repeat the same analysis after first averaging  $R_{OS}^2$  across the alpha term structure for each model, stock, and day, calculating the difference between the number of stocks with a significantly positive and negative  $t$ -statistics at a significance level of 1%. These results are provided in Table 4 in the column denoted by “Avg.”

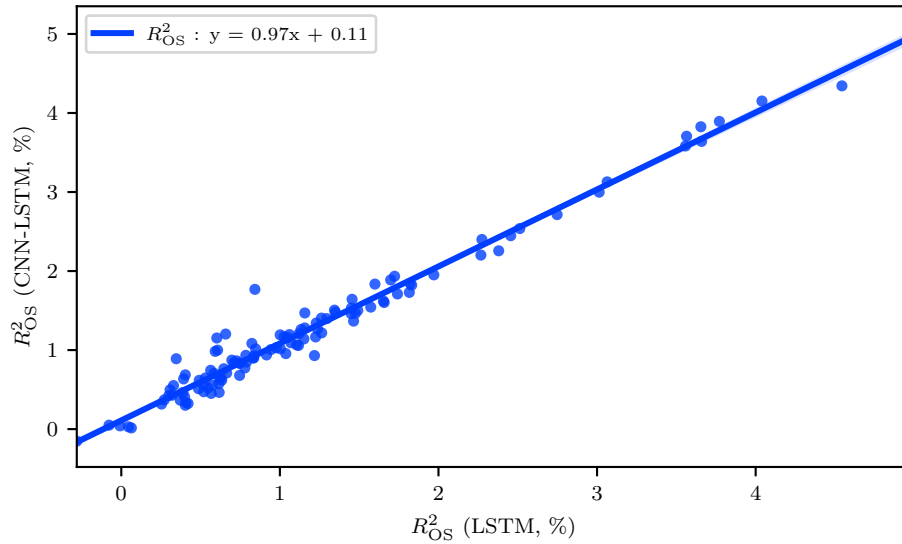


FIGURE 4. Scatter plot of the out-of-sample performance of the LSTM and CNN-LSTM models. Performance is almost identical across all stocks, suggesting the models extract similar features.

Table 4 provides strong support for the claim that models trained on OFs have out-of-sample forecasting ability, with the CNN-LSTM and LSTM coming out slightly ahead of the rest.

**4.1.4. Discussion.** The results above provide support for the fact that ANNs trained on features from the order book can be used to forecast mid-price returns at high frequencies. In particular, we demonstrated that the LSTM-based models trained on OFs inputs perform better than all other model and input combinations we considered. In particular, we observed that when OFs are replaced with LOBs inputs, forecasting performance decreases significantly. Perhaps this is not surprising given that the time series of LOBs are nonstationary. We believe that more sophisticated training techniques are likely to be needed to train ANNs directly on LOBs and achieve superior forecasting performance (Arjovsky et al., 2019).

With OF inputs, our results show that the simple shallow LSTM model performs as well as the deeper and more complex models. Interestingly, even the CNN-LSTM, that uses several convolutional layers on top of an inception module, provides only a small improvement, if one at all. By way of illustration, in Figure 4 we plot the average  $R^2_{OS}$  of the LSTM versus CNN-LSTM models. We observe that the average  $R^2_{OS}$ 's are remarkably similar across all stocks, suggesting the models extract similar features.

In Appendix B.1 we perform a few robustness checks by examining the out-of-sample performance of the models trained on two alternate inputs; in particular, standard OFIs, and LOBs with share volumes only. The results show that the out-of-sample performance of all LSTM-based models are qualitatively similar whether they are trained on OFI or OF inputs. Furthermore, we show that the out-of-sample performance of the models trained on LOBs and LOBs with only share volumes are quite similar, suggesting that bid and ask prices at the first ten levels of the order book do not add predictive power.

Naturally, as the majority of models in this article are based on standard “off-the-shelf” ANN architectures, one would expect that more specialized architectures may deliver better performance. Our results imply that the question of what is the optimal network for return prediction is still an open question. Notably, the more sophisticated CNN-LSTM architecture shows some promise in being able to work directly with LOB inputs. In particular, across all the forecast horizon, for 23 to 45 stocks (out of a total of 115) the CNN-LSTM with LOB inputs exhibits improvements over OF inputs (see, Table 3). Needless to say, from Table 4 we observe that the CNN-LSTM with OF inputs achieves a statistically significant positive  $R_{OS}^2$  across a significantly larger number of symbols than any of the other models in our study (including that of the CNN-LSTM with LOB inputs).

Perhaps somewhat surprising, a key take-away is that as long as an LSTM unit is included, the exact ANN architecture is of secondary importance for short-term return predictability. At the same time, the results in this section provide strong support for the fact that (stationary) OF inputs outperform (non-stationary) LOB inputs.

#### 4.2. Forecasting Performance of the LSTM and Stock Characteristics.

We turn to analyzing how model performance depends on individual stock characteristics at the microstructure level. Based on the results above, where models with an LSTM module trained on OF inputs showed superior performance, we conduct the analysis on a standard “off-the-shelf” LSTM architecture with OF inputs.

We represent the forecasting performance of the LSTM for each stock by its average  $R_{OS}^2$  over the test set. Specifically, for each stock and day, first we average  $R_{OS}^2$  across the alpha term structure. Using the daily averages of  $R_{OS}^2$ 's for each stock, we then determine the grand average over the test set, resulting in a single  $R_{OS}^2$  per symbol.

Following Curato et al. (2015), for the purposes of the analysis in this section, we measure tick size for each stock as the fraction of time that the bid-ask spread is equal to one tick. Figure 5 presents scatter plots of forecasting performance versus tick size, number of updates (calendar time), number of trades (calendar time) and

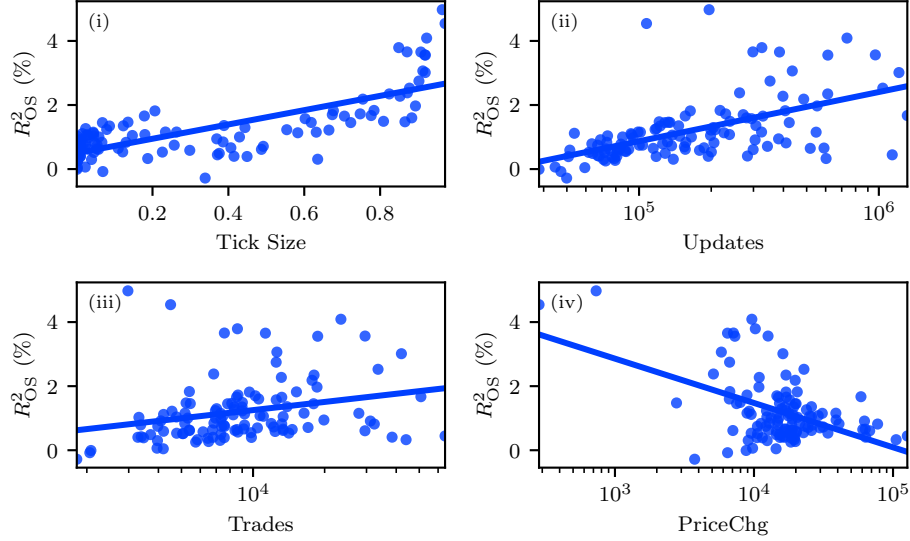


FIGURE 5. Scatter plots with  $R^2_{OS}$ 's from the LSTM model, where the  $R^2_{OS}$ 's are given in percentages. The  $x$ -axis in each panel represents (i) tick size, (ii) number of updates, (iii) number of trades, and (iv) number of price changes, respectively. Note that number of updates, number of price changes, and number of trades are shown on a logarithmic scale. Tick size represents the fraction of time that the bid-ask spread is equal to one tick for each stock (Curato et al., 2015).

number of price changes (calendar time). In panel (i) we observe that a significant proportion of stocks are small-tick and that their  $R^2_{OS}$ 's are clustered in the left hand side of the plot, while the remaining symbols are distributed fairly uniformly. Notably, there is a sharp rise in performance for large-tick stocks. The number of updates, in panel (ii), exhibit a log-linear relationship with  $R^2_{OS}$ , with only minor clustering along the  $x$ -axis. Stocks with a large number of updates show greater variation in forecasting performance. Similarly, the number of trades, in panel (iii), also displays a log-linear relationship with forecasting performance. Lastly, the logarithm of the number of price changes, a proxy for volatility, is negatively correlated with forecasting performance. We interpret this as stocks with lower update frequency and liquidity are less efficient and hence more predictable.

The stock characteristics have high pairwise correlations as seen in Figure 6, where LogUpdates, LogTrades, and LogPriceChg denote the logarithm of the number of updates, trades, and price changes, respectively. Specifically, tick size and the logarithm of updates over price changes have the remarkably high correlation of 0.95. In the next section, we explore how these stock characteristics relate to out-of-sample performance.



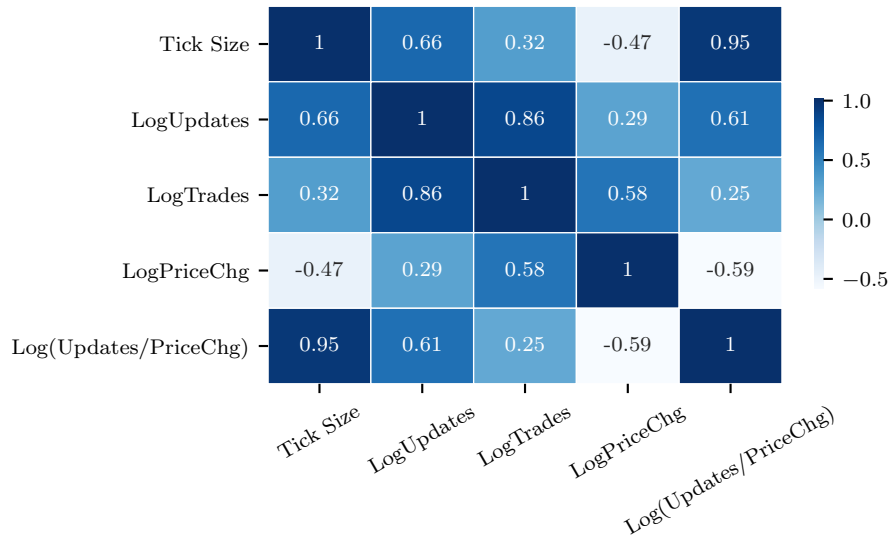


FIGURE 6. Correlation matrix of the stock characteristics. LogUpdates, LogTrades, and LogPriceChg denote the logarithm of the number of updates, trades, and price changes, respectively. Observe that tick size is highly correlated with the logarithm of updates over price changes. Tick size represents the fraction of time that the bid-ask spread is equal to one tick for each stock (Curato et al., 2015).

4.2.1. *Cross-Sectional Regressions.* The first eight columns in Table 5 present the results from univariate regressions with tick size, LogUpdates, LogTrades, and LogPriceChg, where  $t$ - and  $F$ -statistics are calculated using heteroskedasticity-consistent standard errors (White, 1980). As we already discussed the sign of the partial correlations above, here we comment only on the  $t$ -statistics. Noticeably, the  $t$ -statistics are significant at the 1% for all stock characteristics except LogTrades, where the  $t$ -statistic of 2.28 corresponds to a  $p$ -value of 2.3%.

Columns nine and ten display the results from multivariate regressions on all the stock characteristic but tick size. We leave out tick size as we saw above that it is highly correlated with LogUpdates and LogPriceChg. In this setting LogTrades is no longer significant at the 5% level ( $p$ -value = 26.5%). The number of updates and trades are of course closely related. Particularly, some order book updates result in trades, yet it is well-known in the market microstructure literature that the information contained in order book updates is much richer than trades alone (see, for example, Cont et al. (2014) and Bouchaud et al. (2018)). Notice the coefficients for LogUpdates and LogPriceChg are of opposite sign but of similar size, suggesting the regression of  $R_{OS}^2$  on the logarithm of their ratio, Log(Updates/PriceChg); see the eleventh and twelfth columns in Table 5 and Figure 7. While tick size and this ratio are highly correlated, the latter is superior in explaining  $R_{OS}^2$ .

| Variable              | Coeff | <i>t</i> -stat | Coeff  | <i>t</i> -stat | Coeff  | <i>t</i> -stat | Coeff  | <i>t</i> -stat | Coeff   | <i>t</i> -stat | Coeff  | <i>t</i> -stat |
|-----------------------|-------|----------------|--------|----------------|--------|----------------|--------|----------------|---------|----------------|--------|----------------|
| Intercept             | 0.005 | 8.963          | -0.068 | -5.515         | 0.070  | 5.505          | -0.021 | -1.453         | -0.0105 | -1.304         | -0.009 | -7.748         |
| Tick Size             | 0.022 | 9.837          |        |                |        |                |        |                |         |                |        |                |
| LogUpdates            |       |                | 0.007  | 6.288          |        |                |        |                | 0.008   | 6.188          |        |                |
| LogPriceChg           |       |                |        |                | -0.006 | -4.717         |        |                | -0.009  | -12.140        |        |                |
| LogTrades             |       |                |        |                |        |                | 0.004  | 2.277          | 0.002   | 1.116          |        |                |
| Log(Updates/PriceChg) |       |                |        |                |        |                |        |                |         |                | 0.009  | 16.289         |
| Adj. $R^2$            | 0.586 |                | 0.294  |                | 0.229  |                | 0.057  |                | 0.745   |                | 0.746  |                |
| $F$ -stat             | 96.76 |                | 39.54  |                | 22.25  |                | 5.19   |                | 94.90   |                | 265.30 |                |

TABLE 5. Results from multivariate regressions of stock characteristics on forecasting performance ( $R_{OS}^2$ ) from the LSTM model. LogUpdates, LogTrades, LogPriceChg, and Log(Updates/PriceChg) denote the logarithm of the number of updates, trades, price changes, and number of updates per price change, respectively. Tick size represents the fraction of time that the bid-ask spread is equal to one tick for each stock (Curato et al., 2015).  $t$ - and  $F$ -statistics are calculated using heteroskedasticity-consistent standard errors (White, 1980).

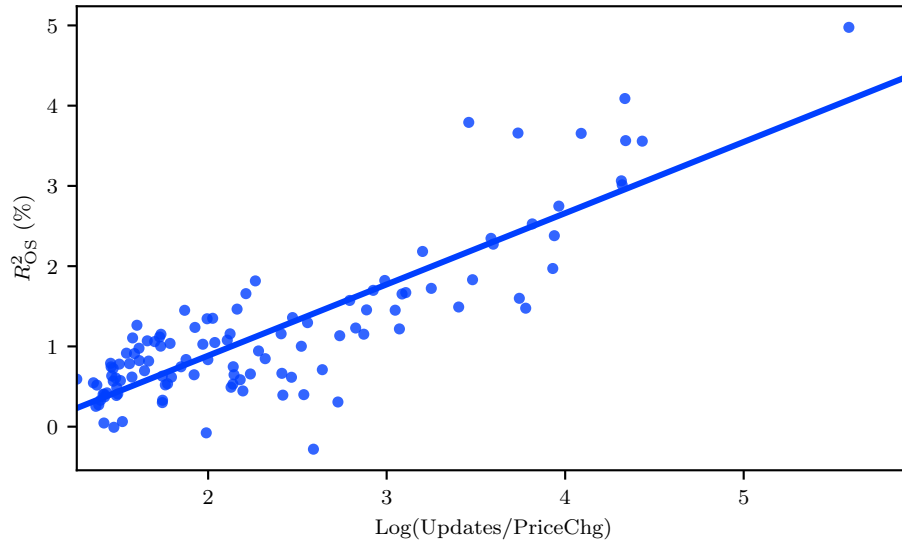


FIGURE 7. Scatter plot of  $R^2_{OS}$ 's and  $\text{Log}(\text{Updates}/\text{PriceChg})$  from the LSTM model trained on OF inputs.

**4.3. Return Predictability At Longer Horizons.** Above we demonstrated there is predictability in mid-price stock returns at short horizons corresponding to the stock specific time scale of up to two average price changes. In this section we explore predictability over longer time spans by extending the forecast horizons in (17) up to ten average price changes. For this analysis, we restrict ourselves to the CNN-LSTM, LSTM, and LSTM-MLP architectures with OF inputs.

Figure 8 depicts the out-of-sample performance, where the curve for each model is produced just as in Section 4.1. We observe that average  $R^2_{OS}$  plateaus at around two average price changes for all models. With a small margin the CNN-LSTM outperforms the two other models up to about 2.3 average price changes. Thereafter, the LSTM-MLP is slightly better, although the difference is minimal.

**4.4. Discussion: Why Is There Predictability?** This article contributes to the emerging literature that uses deep learning in extracting alpha from the most granular information of the order book. While a natural question is *why* this form of predictability exists, to the best of our knowledge there is little supporting theoretical evidence. Although it is generally accepted that order book events (order flow, in particular) impact prices, *specific* details of their interplay is still an open question. In the following, we summarize some of the key findings in the literature and provide some of our conjectures for this phenomenon.

Classical microstructure theories of inventory (Garman, 1976; Amihud et al., 1980; Stoll, 1978; Ho et al., 1981) and asymmetric-information (Glosten et al.,

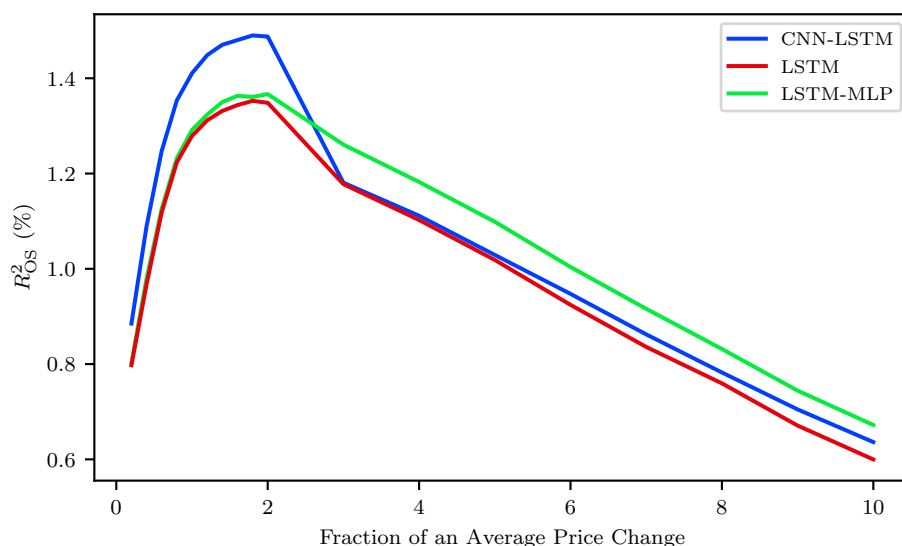


FIGURE 8. Predictive power of the models on a longer horizon (up to 10 average price changes).

1985; Kyle, 1985; Easley et al., 1987) predict that order flow has an impact on prices. For instance, standard inventory models establish that traders acting as market makers adjust their quotes in response to incoming orders, and information-based models predict that trades from informed market participants affect prices. These and related results are also well-established in the empirical literature. For example, Huang et al. (1994) find that differences in quoted depth between the bid and ask sides predict returns, especially over short horizons. Hasbrouck (1988) and Hasbrouck (1991) apply VAR models to separate permanent information effects from transitory inventory effects, showing that information has a significant effect on prices and order flow affects daily returns. Chordia et al. (2002) and Chordia et al. (2004) establish that trade-based order imbalances predict daily returns for individual stocks as well as the overall market. Cao et al. (2009) extend these results up to ten levels of the order book, showing that multilevel imbalances affect returns positively. Needless to say, most of the earlier microstructure literature focus on quote-driven markets, where market makers match orders or fill them from their inventory. In today's electronic markets where trading is conducted via limit order books without any intermediaries, the distinction between market makers and informed market participants is no longer obvious.

Based on their empirical analysis of trade and quote data (best bid and ask at the first level of the order book) of French stocks, Bouchaud et al. (2004) and Bouchaud et al. (2006) suggest that markets are statistically efficient in the sense that mid-price return processes are close to white noise. The authors emphasize two main

opposing effects contributing to this result. First, order flow exhibits long-range correlations due to supply and demand imbalances that take time for the market to digest. Second, while these imbalances alone would lead to price predictability over longer horizons, high-frequency liquidity providers (“market makers”), competing for order flow, cause these mispricings to mean-revert at short horizons.<sup>10</sup> Our empirical results in Section 4.1 and Section 4.3 support that in the intersection of these two counteracting effects there is short-term price predictability.

More recent microstructure literature establishes that not just trades but all updates to the order book are important in understanding price formation; see, for example, the empirical studies of Eisler et al. (2012), Cont et al. (2014), Bouchaud et al. (2018), and Brogaard et al. (2019), and theoretical models of Kaniel et al. (2006), Goettler et al. (2009), and Hoffmann (2014). For instance, Eisler et al. (2012) conduct an empirical study measuring the individual price impact of all order book events, including market orders, limit orders and cancellations. For large-tick stocks, they show that their results are consistent with a model where the impact of all order book events is permanent and non-fluctuating. However, they provide compelling evidence that for small-tick stocks price impact must contain a history-dependent part that represents the internal fluctuations of the order book. Toth et al. (2012) argue that, while liquidity providers are only marginally influenced by their past actions, their current action depend strongly on the recent actions of other market participants. The impact of market orders on prices results from a complex interplay of the broker who pushes the price in the direction of their order flow, as others may trade in the same or different direction. For instance, the authors show that the autocorrelation of order flow in response to a non-price-changing market order is positive on average, suggesting herding amongst brokers. However, in the case of price-changing market orders, Toth et al. (2012) demonstrate that this autocorrelation tends to be negative as other brokers respond with activity in the opposite direction.

An important question is why the return predictability of our models have higher  $R_{OS}^2$ 's for large-tick stocks than those of small-tick stocks. The cross-sectional regression analysis in Section 4.2 sheds some light about how the return predictability varies across stocks. Higher  $R_{OS}^2$  is in part explained by a greater number of order book updates *relative* to that of the number of price changes. A possible explanation might be the following. The number of order book updates over some *characteristic time interval* is a measure of the rate of activity amongst market participants in the order book. Should this characteristic time interval be wall-clock time, or perhaps

<sup>10</sup>Lillo et al. (2004) provide a different explanation, suggesting that the compensating mechanism that leads to uncorrelated returns is that long-range liquidity fluctuations that are correlated with the order flow dampen the otherwise permanent effect of market orders and make the price diffusive.

stock specific? Our results above suggest that the time scale of a stock’s average price change is a sensible choice, and that stocks with a greater number of updates per price change are characterized by a more granular and information-rich price discovery. Additionally, we conjecture that in the case of information-rich stocks (defined as the logarithm of the ratio of updates to price changes) less information is exploited by “traditional” quantitative models as they frequently aggregate information over a fixed time interval that is not stock specific. Therefore, using ANNs to extract unexploited information from the most granular data leads to improved predictability.

While using a different set of models, we believe the market microstructure-based explanation of Gould et al. (2016) also applies to our setting, providing a possible explanation for the difference in return predictability of large- and small-tick stocks.<sup>11</sup> Gould et al. (2016) argue there are two main ways in which mid-price can change. First, a new limit order can arrive inside the bid-ask spread. Second, either the first-level bid or ask volumes,  $v_t^{1,a}, v_t^{1,b}$ , of the order book is fully consumed. Of course, for large-tick stocks the average bid-ask spread will be close to the minimum tick size of \$0.01, diminishing the likelihood of new limit orders arriving inside the bid-ask spread. In this case, positive (negative) mid-price returns are governed only by whether the first-level ask (bid) volume is consumed before the first-level bid (ask) volume. Therefore, it is fair to expect that the bid and ask volumes provide stronger predictive power for large-tick stocks. Gould et al. (2016) also provide an argument based on Nasdaq’s price-time priority rule for why large- and small-tick stocks behave differently, even when the bid-ask spread is not at its minimum. Specifically, traders can place limit orders inside the bid-ask spread to achieve higher priority in the order book. For large-tick stocks, the cost associated with this priority is higher (on a relative basis) than that of small-tick stocks. This incentivizes traders to submit limit orders to the first levels of the order book, resulting in average bid and ask volumes,  $v_t^{1,a}, v_t^{1,b}$ , being greater. In contrast, for small-tick stocks this cost is lower, which make traders more likely to submit limit orders inside the bid-ask spread that decrease the average bid and ask volumes. As before, the greater bid and ask volumes of large-tick stocks (relative to that of small-tick stocks) lead to improved predictability.

## 5. CONCLUSIONS

In this article, we employed deep learning in forecasting high-frequency returns at multiple horizons for 115 stocks traded on Nasdaq using order book information

<sup>11</sup>Gould et al. (2016) use logistic regression classifiers to determine the direction of the subsequent mid-price movement based on OFI for ten stocks on Nasdaq. They find that their model provides a considerable improvement (50-60%) over their benchmark model for large-tick stocks but only a moderate improvement (10-30%) for small-tick stocks.

at the most granular level. While raw order book data can be used as input to the forecasting models, we achieve state-of-the-art predictive accuracy by training simpler “off-the-shelf” artificial neural networks on stationary inputs derived from the order book. Specifically, models trained on order flow significantly outperform most models trained directly on the order book. Using cross-sectional regressions we linked the forecasting performance of the LSTM model to stock characteristics at the market microstructure level, suggesting that “information-rich” stocks can be predicted more accurately by deep learning. Finally, we demonstrated that stock specific forecasts peak at a time scale of about two price changes and declines thereafter.

There are several practical applications for the findings in this article. First, the short-term forecasts can be incorporated into execution algorithms, either as alphas or indirectly in the order submission logic that decides whether to place limit or market orders. Second, the alpha forecasts will be useful in market making systems. In addition, the alphas can be used to design high-frequency trading strategies. Of course, for the latter use case, proper modeling of transaction costs and application of an appropriate execution strategy is critical to their profitability.

Finally, our proposed approach is similar to that of a real-world production setting where the models are updated on a rolling basis. Based on our experience from training the deep learning models in this article across a large number of stocks, we conclude that deploying these models at large scale in practice is fully feasible and no longer a pipe-dream.

#### ACKNOWLEDGEMENTS

We very much appreciate the research assistance of Antonio Briola for this project, especially for creating the illustration in Figure 1. We are grateful to Shenglong Wang for his assistance when developing our data processing and computing environment on NYU’s Greene and Hudson HPC environments. We thank Joan Bruna for insightful suggestions on transfer learning and out-of-distribution generalization, and Will Whitney for thoughtful discussions on casual inference and confounders.

#### APPENDIX A. PREPROCESSING LOBSTER DATA

In this section we discuss the format of the LOBSTER data and summarize the preprocessing steps we performed for this article. For additional information we refer to Bouchaud et al. (2018, Appendix A) and Bugaenko (2020, Appendix C).

LOBSTER provides two files for each date and symbol, the message and order book files. The number of rows in each file is identical and the timestamps are given to nanosecond precision. The message file lists every market order arrival,

limit order arrival and cancellation. We note that the arrival of hidden orders is not provided. The order book file lists the states of the limit order book with each row corresponding to the state after the corresponding event from the message file. It is the order book file which is the primary object of study in this paper.

Inspection of the message file reveals that there are certain clusters of events that require special care. In particular, consider the following three situations:

- (1) Limit order modification which is implemented as a cancellation followed by an immediate new arrival.
- (2) Single market order executing against multiple resting limit orders.
- (3) Auction prints: The auction trade is printed and all the remaining resting limit orders are moved into the limit order book.

Common amongst these situations is that we have one conceptual event which appears as multiple rows in the message file, all with the same timestamp. Consequently, it is critical for modeling purposes that these events are collapsed to avoid artificially inflated prediction accuracy. Therefore, we group the order book data by unique timestamps and take the last entry (they are ordered sequentially within a timestamp by the process which generates this data). This type of processing is standard in the literature using LOBSTER data (see, for example, Bouchaud et al. (2018) and Bugaenko (2020)). In addition, we remove all rows for which the quotes are crossed. As noted in Bouchaud et al. (2018) the occurrence of such events is extremely rare.

Table 6 provides summary statistics after preprocessing the LOBSTER data for the 115 stocks used in this study.

| Ticker | Updates<br>(000) | Trades<br>(000) | Price Changes<br>(000) | Price<br>(USD) | Spread<br>(bps) | Volume<br>(USD MM) |
|--------|------------------|-----------------|------------------------|----------------|-----------------|--------------------|
| AAL    | 398.13           | 13.15           | 10.99                  | 30.65          | 3.88            | 50.29              |
| AAPL   | 1137.36          | 64.19           | 127.86                 | 215.80         | 0.99            | 1156.30            |
| ADBE   | 205.29           | 13.20           | 41.76                  | 283.83         | 4.08            | 194.36             |
| ADI    | 238.35           | 10.70           | 29.23                  | 109.36         | 3.52            | 73.59              |
| ADP    | 128.11           | 7.82            | 20.02                  | 160.65         | 3.62            | 72.97              |
| ADSK   | 118.22           | 8.34            | 24.27                  | 161.21         | 5.48            | 74.96              |
| ALGN   | 80.86            | 6.78            | 20.01                  | 251.14         | 9.68            | 81.68              |
| ALXN   | 93.19            | 7.47            | 18.08                  | 117.26         | 7.45            | 52.07              |
| AMAT   | 611.97           | 18.05           | 17.15                  | 47.36          | 2.62            | 91.72              |
| AMD    | 1213.04          | 42.06           | 16.26                  | 31.33          | 3.64            | 343.63             |
| AMGN   | 137.56           | 11.06           | 25.61                  | 198.36         | 3.85            | 138.33             |
| AMZN   | 304.76           | 31.14           | 64.23                  | 1795.51        | 2.59            | 1531.40            |
| ANSS   | 63.55            | 3.37            | 15.22                  | 206.76         | 9.39            | 25.86              |
| ASML   | 147.63           | 3.31            | 21.21                  | 223.92         | 7.06            | 46.42              |
| ATVI   | 423.01           | 17.97           | 20.25                  | 49.87          | 2.81            | 91.82              |
| AVGO   | 136.68           | 12.20           | 32.10                  | 289.33         | 4.62            | 182.39             |
| BIDU   | 155.90           | 13.37           | 26.50                  | 132.58         | 4.79            | 129.79             |
| BIIB   | 88.20            | 9.80            | 23.17                  | 265.36         | 6.01            | 129.65             |
| BKNG   | 51.44            | 4.20            | 15.00                  | 1881.52        | 8.68            | 169.08             |
| BMRN   | 61.69            | 5.08            | 10.81                  | 82.87          | 10.20           | 25.70              |
| CDNS   | 128.56           | 7.32            | 15.40                  | 64.99          | 4.28            | 32.49              |
| CDW    | 53.73            | 4.20            | 9.73                   | 112.53         | 7.93            | 28.02              |

Continued on next page



| Ticker | Updates<br>(000) | Trades<br>(000) | Price Changes<br>(000) | Price<br>(USD) | Spread<br>(bps) | Volume<br>(USD MM) |
|--------|------------------|-----------------|------------------------|----------------|-----------------|--------------------|
| CERN   | 117.85           | 7.57            | 10.59                  | 66.41          | 3.53            | 38.58              |
| CHKP   | 67.19            | 3.98            | 10.82                  | 114.42         | 6.51            | 27.00              |
| CHTR   | 80.97            | 6.75            | 19.21                  | 400.68         | 6.22            | 111.71             |
| CMCSA  | 612.78           | 18.70           | 7.44                   | 42.40          | 2.58            | 128.95             |
| COST   | 125.41           | 9.21            | 26.87                  | 264.93         | 3.26            | 120.40             |
| CPRT   | 80.99            | 4.77            | 9.66                   | 73.53          | 5.03            | 23.75              |
| CSCO   | 736.33           | 23.41           | 9.81                   | 50.37          | 2.17            | 191.94             |
| CSGP   | 38.27            | 2.08            | 9.03                   | 536.05         | 23.06           | 34.75              |
| CSX    | 294.56           | 12.52           | 18.20                  | 72.07          | 2.35            | 78.23              |
| CTAS   | 64.05            | 3.71            | 14.75                  | 237.20         | 7.29            | 34.05              |
| CTSH   | 271.85           | 10.22           | 14.73                  | 64.84          | 2.39            | 58.60              |
| CTXS   | 103.49           | 7.60            | 12.32                  | 102.47         | 3.55            | 52.46              |
| DISH   | 138.93           | 7.27            | 9.16                   | 34.30          | 4.95            | 21.35              |
| DLTR   | 132.57           | 8.14            | 15.42                  | 102.30         | 4.23            | 57.93              |
| EA     | 198.67           | 13.38           | 26.25                  | 96.82          | 4.19            | 95.90              |
| EBAY   | 435.54           | 12.59           | 5.91                   | 37.05          | 2.98            | 66.41              |
| EXC    | 298.32           | 7.58            | 7.21                   | 47.35          | 2.45            | 37.55              |
| EXPE   | 122.44           | 8.33            | 16.93                  | 122.62         | 4.45            | 62.15              |
| FAST   | 229.64           | 8.64            | 8.99                   | 44.16          | 3.47            | 34.60              |
| FB     | 602.54           | 44.01           | 106.38                 | 184.08         | 1.71            | 622.29             |
| FISV   | 178.66           | 12.38           | 20.43                  | 97.41          | 3.14            | 90.26              |
| FOX    | 199.41           | 4.56            | 9.31                   | 37.81          | 4.33            | 19.34              |
| FOXA   | 239.37           | 9.02            | 8.03                   | 38.22          | 3.39            | 44.54              |
| GILD   | 407.04           | 15.22           | 20.67                  | 65.53          | 2.22            | 96.45              |
| GLIBA  | 47.21            | 2.06            | 6.55                   | 61.12          | 15.97           | 7.51               |
| GOOG   | 590.59           | 13.38           | 64.96                  | 1206.29        | 4.71            | 468.31             |
| GOOGL  | 517.61           | 14.61           | 62.70                  | 1208.90        | 4.40            | 445.79             |
| HAS    | 73.34            | 5.16            | 11.42                  | 101.28         | 6.61            | 30.45              |
| HOLX   | 134.48           | 5.45            | 7.55                   | 48.02          | 3.85            | 20.87              |
| HSIC   | 99.05            | 5.18            | 9.01                   | 66.23          | 5.41            | 23.73              |
| IDXX   | 67.22            | 3.39            | 16.85                  | 251.26         | 9.72            | 30.08              |
| ILMN   | 79.51            | 6.50            | 20.37                  | 310.12         | 7.77            | 84.54              |
| INCY   | 72.65            | 5.39            | 12.91                  | 81.55          | 8.74            | 26.16              |
| INTC   | 966.81           | 29.58           | 12.86                  | 52.13          | 2.10            | 231.35             |
| INTU   | 100.24           | 7.37            | 23.84                  | 257.26         | 5.30            | 88.90              |
| ISRG   | 78.95            | 5.84            | 20.09                  | 535.71         | 7.83            | 94.48              |
| JBHT   | 73.90            | 4.76            | 12.57                  | 104.88         | 7.74            | 28.07              |
| JD     | 552.74           | 18.58           | 10.95                  | 29.94          | 3.79            | 95.11              |
| KHC    | 351.72           | 12.51           | 6.75                   | 32.58          | 3.48            | 58.06              |
| KLAC   | 94.44            | 7.33            | 19.12                  | 136.17         | 6.19            | 53.08              |
| LBTYA  | 217.71           | 5.40            | 6.73                   | 24.95          | 5.39            | 13.11              |
| LBTYK  | 262.49           | 6.83            | 5.15                   | 24.16          | 4.99            | 19.60              |
| LILAK  | 49.89            | 1.81            | 3.77                   | 18.09          | 15.92           | 2.63               |
| LRCX   | 154.50           | 10.43           | 30.42                  | 215.34         | 5.48            | 111.39             |
| LULU   | 92.51            | 8.25            | 19.44                  | 184.49         | 6.34            | 87.43              |
| MAR    | 116.61           | 6.94            | 17.30                  | 130.38         | 4.51            | 54.67              |
| MCHP   | 146.21           | 8.99            | 19.50                  | 91.11          | 4.95            | 51.90              |
| MDLZ   | 385.19           | 11.27           | 6.57                   | 51.78          | 2.16            | 68.01              |
| MELI   | 68.15            | 3.28            | 16.99                  | 538.46         | 19.44           | 72.08              |
| MNST   | 207.65           | 9.02            | 12.41                  | 59.63          | 3.14            | 45.60              |
| MSFT   | 1314.51          | 50.80           | 59.44                  | 132.70         | 0.96            | 674.33             |
| MU     | 1038.48          | 33.55           | 23.06                  | 43.55          | 2.64            | 224.59             |
| MXIM   | 165.32           | 6.96            | 13.37                  | 57.14          | 4.29            | 28.77              |
| MYL    | 280.72           | 10.56           | 6.72                   | 22.25          | 5.33            | 30.69              |
| NFLX   | 299.09           | 29.56           | 69.40                  | 329.25         | 3.92            | 554.70             |
| NTAP   | 186.58           | 9.14            | 16.83                  | 60.89          | 4.14            | 40.97              |
| NTES   | 59.40            | 4.19            | 14.83                  | 268.10         | 13.15           | 55.21              |
| NVDA   | 410.14           | 32.36           | 78.34                  | 179.73         | 3.12            | 388.83             |
| NXPI   | 156.79           | 11.93           | 21.49                  | 103.13         | 5.01            | 88.60              |
| ORLY   | 71.82            | 5.06            | 18.57                  | 393.07         | 7.90            | 69.74              |
| PAYX   | 204.00           | 7.03            | 15.93                  | 81.79          | 2.86            | 38.72              |
| PCAR   | 131.38           | 6.85            | 13.03                  | 70.63          | 3.82            | 34.43              |

Continued on next page

| Ticker | Updates<br>(000) | Trades<br>(000) | Price Changes<br>(000) | Price<br>(USD) | Spread<br>(bps) | Volume<br>(USD MM) |
|--------|------------------|-----------------|------------------------|----------------|-----------------|--------------------|
| PEP    | 307.10           | 13.89           | 26.13                  | 128.67         | 1.73            | 125.57             |
| PYPL   | 381.85           | 19.86           | 39.32                  | 105.65         | 2.21            | 164.14             |
| QCOM   | 547.61           | 27.86           | 31.30                  | 73.04          | 2.23            | 213.91             |
| QRTEA  | 121.32           | 5.23            | 2.79                   | 13.54          | 9.75            | 9.53               |
| REGN   | 72.53            | 5.74            | 18.86                  | 344.93         | 9.32            | 70.71              |
| ROST   | 155.81           | 8.53            | 17.27                  | 103.03         | 3.85            | 55.34              |
| SBUX   | 485.99           | 17.70           | 19.99                  | 82.04          | 1.63            | 139.81             |
| SGEN   | 44.67            | 3.95            | 9.96                   | 82.34          | 15.15           | 19.56              |
| SIRI   | 107.42           | 4.50            | 0.29                   | 6.21           | 16.69           | 25.20              |
| SNPS   | 85.39            | 5.32            | 15.31                  | 125.01         | 5.77            | 35.22              |
| SPLK   | 84.00            | 7.54            | 19.09                  | 129.00         | 8.36            | 57.97              |
| STX    | 226.02           | 9.21            | 14.74                  | 50.18          | 3.67            | 38.19              |
| SWKS   | 114.57           | 8.55            | 16.98                  | 86.36          | 5.71            | 46.25              |
| TMUS   | 194.31           | 9.84            | 15.56                  | 75.70          | 3.08            | 60.40              |
| TSLA   | 283.15           | 38.43           | 65.03                  | 292.35         | 4.66            | 724.21             |
| TTWO   | 101.33           | 7.31            | 18.13                  | 112.77         | 6.62            | 51.14              |
| TXN    | 324.28           | 16.38           | 39.16                  | 116.63         | 2.43            | 136.22             |
| UAL    | 163.59           | 9.65            | 17.19                  | 86.65          | 3.98            | 59.90              |
| ULTA   | 77.25            | 6.45            | 19.19                  | 297.27         | 8.64            | 79.56              |
| VOD    | 195.93           | 2.98            | 0.74                   | 18.56          | 5.62            | 14.53              |
| VRSK   | 71.10            | 3.96            | 12.71                  | 142.97         | 5.62            | 28.14              |
| VRSN   | 69.03            | 4.10            | 15.10                  | 191.87         | 6.80            | 34.27              |
| VRTX   | 76.14            | 6.16            | 17.19                  | 187.81         | 7.44            | 58.90              |
| WBA    | 328.50           | 13.20           | 15.18                  | 57.81          | 2.54            | 75.19              |
| WDAY   | 87.49            | 8.63            | 20.57                  | 185.12         | 8.02            | 86.66              |
| WDC    | 343.08           | 17.03           | 24.69                  | 51.91          | 3.89            | 77.10              |
| WLTW   | 50.77            | 3.47            | 11.74                  | 185.22         | 8.16            | 27.11              |
| WYNN   | 90.56            | 8.39            | 19.15                  | 123.37         | 7.61            | 64.33              |
| XEL    | 325.18           | 8.60            | 10.32                  | 59.35          | 2.06            | 44.25              |
| XLNX   | 200.22           | 14.14           | 34.38                  | 107.30         | 4.31            | 103.57             |
| XRAY   | 83.07            | 5.41            | 7.11                   | 52.32          | 4.35            | 21.67              |

TABLE 6. Summary statistics of the 115 stocks from Nasdaq used in this study. The data is sourced from LOBSTER, covering the time period January 1, 2019 through January 31, 2020. Updates, trades, and price changes represent the average number of order book updates, trades and price changes in thousands per day. Price, spread, and volume denote the average price in dollars, bid-ask spread in basis points, and daily volume in dollars, respectively.

## APPENDIX B. SUPPLEMENTARY RESULTS

**B.1. Alternate Inputs.** We report on the out-of-sample performance of our models trained on two alternate inputs: (i) standard OFIs (see, equations (5)), and (ii) LOBs with share volumes only (i.e. inputs of the form of equation (1) where bid and ask prices have been removed). Just as for the OFs in the main article, the different sizes of these inputs necessitate small adjustments of the CNN-LSTM architecture. For instance, the CNN-LSTM with OFI inputs is made up of block 3 through block 5 only, with the input to the first layer being of size  $100 \times 10 \times 1$ .

Figure 9 depicts the out-of-sample performance for the models with OFIs (left panel) and LOBs without prices (right panel). Comparing the left panels of Figure 2 and Figure 9, we observe that the out-of-sample performance of all LSTM-based models are qualitatively similar whether trained on OFI or OF inputs. However,

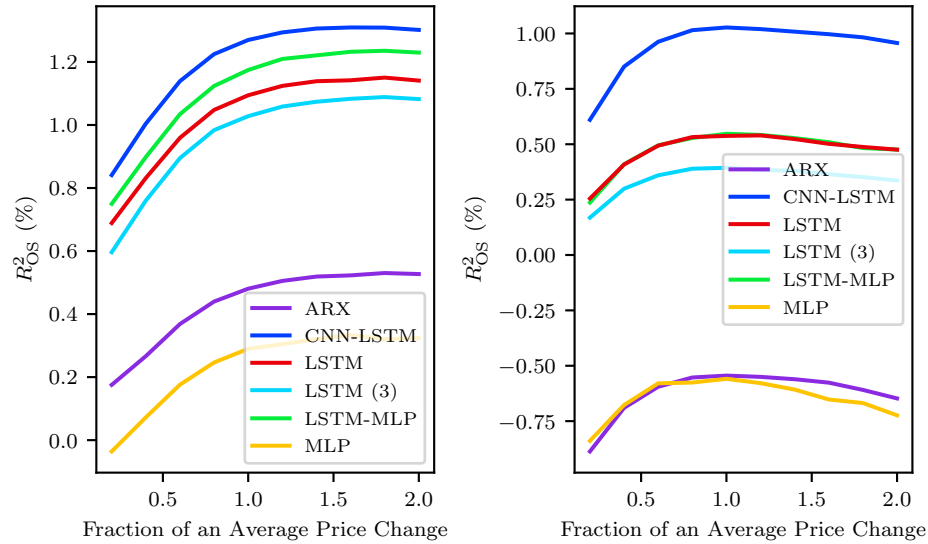


FIGURE 9. Results from robustness checks of the out-of-sample forecasting performance of models at different horizons from 10 levels of standard OFIs (left panel) and order book states with bid and ask prices removed (right panel). Model performance is measured as the average  $R^2_{OS}$  across days and stocks. Horizons are given as the fraction of an average price change for each stock. Each model is trained using a rolling-window out-of-sample methodology across 11 months of data.

when the ARX and MLP are trained on OFI instead of OF inputs, their  $R^2_{OS}$  improve from about 0.1 to 0.5 and 0.25 to 0.3, respectively. This improvement is likely due to the reduction of model parameters when going from OF to OFI inputs. Additional tuning of the MLP hyperparameters and customized feature engineering for the ARX model are interesting topics that will likely further improve their performance. However, as they are outside the scope of this article we do not explore them here.

Examining the right panels of Figure 2 and Figure 9, it is clear that the out-of-sample performance of the models trained on full LOBs or LOBs with share volumes only are qualitatively similar. This suggest that bid and ask prices are not confounding factors for returns and volumes (Pearl, 2009).

**B.2. Short-Term Return Predictability and Its Dependence on the Training Window.** In the training of the models in the main article, we use a fixed lookback window of  $W = 100$  for all stocks (see, Section 3.2 for details). Here we revisit this assumption, examining the performance of dynamic lookback windows that are specific to each stock.

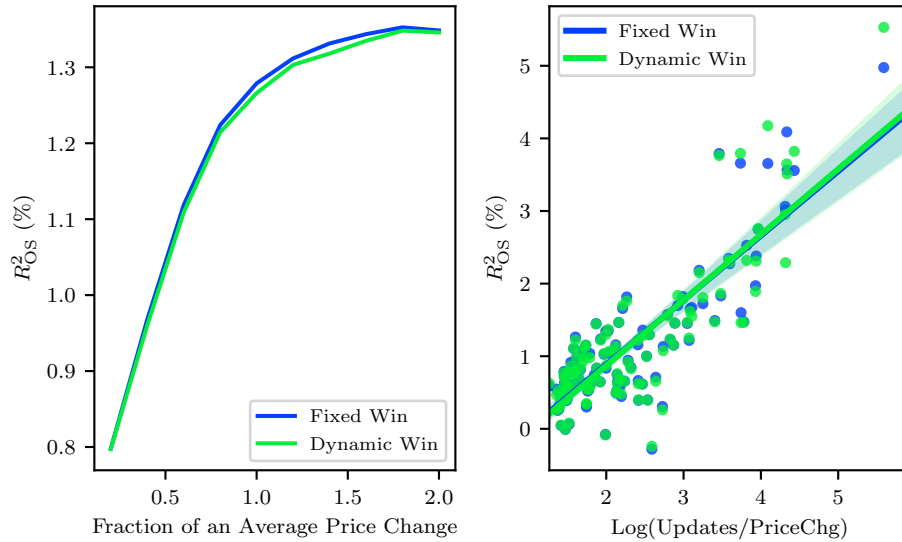


FIGURE 10. The left panel shows the out-of-sample forecasting performance of the LSTM model trained OF inputs with a fixed window length of 100 updates (Fixed Win, in blue), as in the main article, and a stock specific window lengths (Dynamic Win, in green). Model performance is measured as the average  $R^2_{OS}$  across days and stocks. Horizons are given as the fraction of an average price change for each stock. Each model is trained using a rolling-window out-of-sample methodology across 11 months of data. The right panel provides a scatter plot of  $R^2_{OS}$ 's and  $\text{Log}(\text{Updates}/\text{PriceChg})$  from the LSTM model trained on OF inputs with a fixed window length of 100 updates (in blue) and a stock specific window length (in green).

We choose the stock specific windows as follows. First, for each stock we determine the average number of updates that occur during two price changes and multiply this number by three. If the result is less than or equal to 300, we set this to be the stock specific window size; if it is greater than 300, we cap the stock specific window size to 300. This results in a median stock specific window length of 50 updates, and 25th and 75th percentiles of 29.5 and 107 updates, respectively.

Figure 10 compares fixed and dynamic lookback windows for the LSTM model trained on OF inputs for all stocks. We train and report the out-of-sample performance in the same way as in the main article. The left panel illustrates that the model performance of the two different kinds of training windows are quite similar. The right panel provides a scatter plot of  $R^2_{OS}$ 's and  $\text{Log}(\text{Updates}/\text{PriceChg})$  of the two approaches. These results suggest that window length is less important as a driver of out-of-sample predictive performance.

## REFERENCES

- Abadi, Martín et al. (2015). *TensorFlow: Large-Scale Machine Learning on Heterogeneous Systems*. URL: <https://www.tensorflow.org/>.
- Abergel, Frédéric, Marouane Anane, Anirban Chakraborti, Aymen Jedidi, and Ioane Muni Toke (2016). *Limit Order Books*. Cambridge University Press.
- Amihud, Yakov and Haim Mendelson (1980). “Dealership Market: Market-Making With Inventory”. In: *Journal Of Financial Economics* 8.1, pp. 31–53.
- Arjovsky, Martin, Léon Bottou, Ishaan Gulrajani, and David Lopez-Paz (2019). “Invariant Risk Minimization”. In: *arXiv preprint arXiv:1907.02893*.
- Bahdanau, Dzmitry, Kyunghyun Cho, and Yoshua Bengio (2014). “Neural Machine Translation By Jointly Learning To Align And Translate”. In: *arXiv preprint arXiv:1409.0473*.
- Bengio, Yoshua (2012). “Deep Learning Of Representations For Unsupervised And Transfer Learning”. In: *Proceedings Of ICML Workshop On Unsupervised And Transfer Learning*. JMLR Workshop and Conference Proceedings, pp. 17–36.
- Bouchaud, Jean-Philippe, Julius Bonart, Jonathan Donier, and Martin Gould (2018). *Trades, Quotes and Prices: Financial Markets Under the Microscope*. Cambridge University Press.
- Bouchaud, Jean-Philippe, Yuval Gefen, Marc Potters, and Matthieu Wyart (2004). “Fluctuations And Response In Financial Markets: The Subtle Nature Of ‘Random’ Price Changes”. In: *Quantitative Finance* 4.2, pp. 176–190.
- Bouchaud, Jean-Philippe, Julien Kockelkoren, and Marc Potters (2006). “Random Walks, Liquidity Molasses And Critical Response In Financial Markets”. In: *Quantitative Finance* 6.2, pp. 115–123.
- Briola, Antonio, Jeremy Turiel, and Tomaso Aste (2020). *Deep Learning Modeling Of Limit Order Book: A Comparative Perspective*. arXiv: 2007 . 07319 [q-fin.TR].
- Brogaard, Jonathan, Terrence Hendershott, and Ryan Riordan (2019). “Price Discovery Without Trading: Evidence From Limit Orders”. In: *The Journal of Finance* 74.4, pp. 1621–1658.
- Bugaenko, Anastasia (2020). *Empirical Study of Market Impact Conditional on Order-Flow Imbalance*. arXiv: 2004.08290 [q-fin.CP].
- Cao, Charles, Oliver Hansch, and Xiaoxin Wang (2009). “The Information Content Of An Open Limit-Order Book”. In: *Journal of Futures Markets: Futures, Options, and Other Derivative Products* 29.1, pp. 16–41.
- Cho, Kyunghyun, Bart Van Merriënboer, Caglar Gulcehre, Dzmitry Bahdanau, Fethi Bougares, Holger Schwenk, and Yoshua Bengio (2014). “Learning Phrase

- Representations Using RNN Encoder-Decoder For Statistical Machine Translation". In: *arXiv preprint arXiv:1406.1078*.
- Chollet, François et al. (2015). *Keras*. <https://github.com/fchollet/keras>.
- Chordia, Tarun, Richard Roll, and Avanidhar Subrahmanyam (2002). "Order Imbalance, Liquidity, And Market Returns". In: *Journal Of Financial Economics* 65.1, pp. 111–130.
- Chordia, Tarun and Avanidhar Subrahmanyam (2004). "Order Imbalance And Individual Stock Returns: Theory And Evidence". In: *Journal of Financial Economics* 72.3, pp. 485–518.
- Cont, Rama (2001). "Empirical Properties Of Asset Returns: Stylized Facts And Statistical Issues". In: *Quantitative Finance* 1.2, p. 223.
- Cont, Rama, Arseniy Kukanov, and Sasha Stoikov (2014). "The Price Impact Of Order Book Events". In: *Journal Of Financial Econometrics* 12.1, pp. 47–88.
- Curato, Gianbiagio and Fabrizio Lillo (2015). "How Tick Size Affects the High Frequency Scaling of Stock Return Distributions". In: *Financial Econometrics and Empirical Market Microstructure*. Springer, pp. 55–76.
- Devlin, Jacob, Ming-Wei Chang, Kenton Lee, and Kristina Toutanova (2018). "BERT: Pre-Training Of Deep Bidirectional Transformers For Language Understanding". In: *arXiv preprint arXiv:1810.04805*.
- Donahue, Jeffrey, Lisa Anne Hendricks, Sergio Guadarrama, Marcus Rohrbach, Subhashini Venugopalan, Kate Saenko, and Trevor Darrell (2015). "Long-Term Recurrent Convolutional Networks For Visual Recognition And Description". In: *Proceedings Of The IEEE Conference On Computer Vision And Pattern Recognition*, pp. 2625–2634.
- Easley, David and Maureen O'Hara (1987). "Price, Trade Size, And Information In Securities Markets". In: *Journal Of Financial Economics* 19.1, pp. 69–90.
- Eisler, Zoltan, Jean-Philippe Bouchaud, and Julien Kockelkoren (2012). "The Price Impact Of Order Book Events: Market Orders, Limit Orders And Cancellations". In: *Quantitative Finance* 12.9, pp. 1395–1419.
- Elmsili, Bilal and Benaceur Outtaj (2018). "Artificial Neural Networks Applications In Economics And Management Research: An Exploratory Literature Review". In: *2018 4th International Conference on Optimization and Applications (ICOA)*. IEEE, pp. 1–6.
- Fawaz, Hassan Ismail, Germain Forestier, Jonathan Weber, Lhassane Idoumghar, and Pierre-Alain Muller (2019). "Deep Learning For Time Series Classification: A Review". In: *Data Mining and Knowledge Discovery* 33.4, pp. 917–963.
- Friedman, Jerome, Trevor Hastie, and Robert Tibshirani (2017). *The Elements Of Statistical Learning*. 12th Printing. Springer Series In Statistics New York.

- Garman, Mark B. (1976). “Market Microstructure”. In: *Journal Of Financial Economics* 3.3, pp. 257–275.
- Gers, Felix A., Jürgen Schmidhuber, and Fred Cummins (2000). “Learning To Forget: Continual Prediction With LSTM”. In: *Neural Computation* 12.10, pp. 2451–2471.
- Glosten, Lawrence R. and Paul R. Milgrom (1985). “Bid, Ask And Transaction Prices In A Specialist Market With Heterogeneously Informed Traders”. In: *Journal Of Financial Economics* 14.1, pp. 71–100.
- Goettler, Ronald L., Christine A. Parlour, and Uday. Rajan (2009). “Informed Traders And Limit Order Markets”. In: *Journal of Financial Economics* 93.1, pp. 67–87.
- Goodfellow, Ian, Yoshua Bengio, and Aaron Courville (2016). *Deep Learning*. MIT press.
- Gould, Martin D. and Julius Bonart (2016). “Queue Imbalance As A One-Tick-Ahead Price Predictor In A Limit Order Book”. In: *Market Microstructure and Liquidity* 2.2, p. 1650006.
- Gould, Martin D., Mason A. Porter, Stacy Williams, Mark McDonald, Daniel J. Fenn, and Sam D. Howison (2013). “Limit Order Books”. In: *Quantitative Finance* 13.11, pp. 1709–1742.
- Graves, Alex (2013). “Generating Sequences With Recurrent Neural Networks”. In: *arXiv preprint arXiv:1308.0850*.
- Graves, Alex, Abdel-Rahman Mohamed, and Geoffrey Hinton (2013). “Speech Recognition With Deep Recurrent Neural Networks”. In: *2013 IEEE International Conference On Acoustics, Speech And Signal Processing*. IEEE, pp. 6645–6649.
- Greff, Klaus, Rupesh K. Srivastava, Jan Koutník, Bas R. Steunebrink, and Jürgen Schmidhuber (2016). “LSTM: A Search Space Odyssey”. In: *IEEE Transactions On Neural Networks And Learning Systems* 28.10, pp. 2222–2232.
- Hamilton, James Douglas (1994). *Time Series Analysis*. Princeton University Press.
- Hasbrouck, Joel (1988). “Trades, Quotes, Inventories, And Information”. In: *Journal Of Financial Economics* 22.2, pp. 229–252.
- (1991). “Measuring The Information Content Of Stock Trades”. In: *The Journal of Finance* 46.1, pp. 179–207.
- Hasbrouck, Joel and Gideon Saar (2013). “Low-Latency Trading”. In: *Journal of Financial Markets* 16.4, pp. 646–679.
- Ho, Thomas and Hans R. Stoll (1981). “Optimal Dealer Pricing Under Transactions And Return Uncertainty”. In: *Journal Of Financial Economics* 9.1, pp. 47–73.
- Hochreiter, Sepp and Jürgen Schmidhuber (1997). “Long Short-Term Memory”. In: *Neural Computation* 9.8, pp. 1735–1780.

- Hoffmann, Peter (2014). “A Dynamic Limit Order Market With Fast And Slow Traders”. In: *Journal of Financial Economics* 113.1, pp. 156–169.
- Hornik, Kurt (1991). “Approximation Capabilities Of Multilayer Feedforward Networks”. In: *Neural Networks* 4.2, pp. 251–257.
- Huang, Roger D. and Hans R. Stoll (1994). “Market Microstructure And Stock Return Predictions”. In: *The Review of Financial Studies* 7.1, pp. 179–213.
- Huang, Ruihong and Tomas Polak (2011). “LOBSTER: Limit Order Book Reconstruction System”. In: *Available at SSRN 1977207*.
- Jaisson, Thibault and Mathieu Rosenbaum (2016). “Rough Fractional Diffusions As Scaling Limits Of Nearly Unstable Heavy Tailed Hawkes Processes”. In: *The Annals of Applied Probability* 26.5, pp. 2860–2882.
- Jozefowicz, Rafal, Wojciech Zaremba, and Ilya Sutskever (2015). “An Empirical Exploration Of Recurrent Network Architectures”. In: *International Conference On Machine Learning*. PMLR, pp. 2342–2350.
- Kaniel, Ron and Hong Liu (2006). “So What Orders Do Informed Traders Use?” In: *The Journal of Business* 79.4, pp. 1867–1913.
- Kercheval, Alec N. and Yuan Zhang (2015). “Modelling High-Frequency Limit Order Book Dynamics With Support Vector Machines”. In: *Quantitative Finance* 15.8, pp. 1315–1329.
- Keskar, Nitish Shirish, Dheevatsa Mudigere, Jorge Nocedal, Mikhail Smelyanskiy, and Ping Tak Peter Tang (2017). *On Large-Batch Training for Deep Learning: Generalization Gap and Sharp Minima*. arXiv: 1609.04836 [cs.LG].
- Kim, Yoon, Yacine Jernite, David Sontag, and Alexander Rush (2016). “Character-Aware Neural Language Models”. In: *Proceedings Of The AAAI Conference On Artificial Intelligence*. Vol. 30. 1.
- Kingma, Diederik P. and Jimmy Ba (2014). *Adam: A Method for Stochastic Optimization*. arXiv: 1412.6980 [cs.LG].
- Kolm, Petter N. and Nicholas Westray (2021). “Information Content Of Cross-Sectional Multilevel Order Flow Imbalance”. In preparation.
- Krizhevsky, Alex, Ilya Sutskever, and Geoffrey E. Hinton (2012). “Imagenet Classification With Deep Convolutional Neural Networks”. In: *Advances In Neural Information Processing Systems* 25, pp. 1097–1105.
- Kyle, Albert S. (1985). “Continuous Auctions And Insider Trading”. In: *Econometrica* 53.6, pp. 1315–1335.
- LeCun, Yann, Yoshua Bengio, and Geoffrey Hinton (2015). “Deep Learning”. In: *Nature* 521.7553, pp. 436–444.
- Li, Yuhong and Weihua Ma (2010). “Applications Of Artificial Neural Networks In Financial Economics: A Survey”. In: *2010 International Symposium On Computational Intelligence And Design*. Vol. 1. IEEE, pp. 211–214.



- Lillo, Fabrizio and J. Doyne Farmer (2004). “The Long Memory Of The Efficient Market”. In: *Studies In Nonlinear Dynamics & Econometrics* 8.3.
- Liu, Lily Y., Andrew J. Patton, and Kevin Sheppard (2015). “Does Anything Beat 5-Minute RV? A Comparison Of Realized Measures Across Multiple Asset Classes”. In: *Journal of Econometrics* 187.1, pp. 293–311.
- Luo, Wei and Feng Yu (2019). “Recurrent Highway Networks With Grouped Auxiliary Memory”. In: *IEEE Access* 7, pp. 182037–182049.
- Mäkinen, Ymir, Juho Kanninen, Moncef Gabbouj, and Alexandros Iosifidis (2019). “Forecasting Jump Arrivals In Stock Prices: New Attention-Based Network Architecture Using Limit Order Book Data”. In: *Quantitative Finance* 19.12, pp. 2033–2050.
- Mertens, Luca, Alberto Ciacchi, Fabrizio Lillo, and Giulia Livieri (2019). “Liquidity Fluctuations And The Latent Dynamics Of Price Impact”. In: *Available at SSRN* 3214744.
- Mnih, Volodymyr, Nicolas Heess, Alex Graves, and Koray Kavukcuoglu (2014). “Recurrent Models Of Visual Attention”. In: *arXiv preprint arXiv:1406.6247*.
- Ntakaris, Adamantios, Martin Magris, Juho Kanninen, Moncef Gabbouj, and Alexandros Iosifidis (2018). “Benchmark Dataset For Mid-Price Forecasting Of Limit Order Book Data With Machine Learning Methods”. In: *Journal of Forecasting* 37.8, pp. 852–866.
- Ozbayoglu, Ahmet Murat, Mehmet Ugur Gudelek, and Omer Berat Sezer (2020). “Deep Learning For Financial Applications : A Survey”. In: *Applied Soft Computing* 93, p. 106384.
- Pan, Sinno Jialin and Qiang Yang (2009). “A Survey On Transfer Learning”. In: *IEEE Transactions On Knowledge And Data Engineering* 22.10, pp. 1345–1359.
- Pascanu, Razvan, Caglar Gulcehre, Kyunghyun Cho, and Yoshua Bengio (2013). “How To Construct Deep Recurrent Neural Networks”. In: *arXiv preprint arXiv:1312.6026*.
- Passalis, Nikolaos, Anastasios Tefas, Juho Kanninen, Moncef Gabbouj, and Alexandros Iosifidis (2020). “Temporal Logistic Neural Bag-Of-Features For Financial Time Series Forecasting Leveraging Limit Order Book Data”. In: *Pattern Recognition Letters* 136, pp. 183–189.
- Patton, Andrew J. (2011). “Data-Based Ranking Of Realised Volatility Estimators”. In: *Journal of Econometrics* 161.2, pp. 284–303.
- Pearl, Judea (2009). *Causality*. Cambridge University Press.
- Rahimikia, Eghbal and Ser-Huang Poon (2021). “Machine Learning For Realised Volatility Forecasting”. In: *Available at SSRN* 3707796.
- Rumelhart, David E., Geoffrey E. Hinton, and Ronald J. Williams (1986). “Learning Representations By Back-Propagating Errors”. In: *Nature* 323.6088, pp. 533–536.

- Sainath, Tara N., Oriol Vinyals, Andrew Senior, and Haşim Sak (2015). “Convolutional, Long Short-Term Memory, Fully Connected Deep Neural Networks”. In: *2015 IEEE International Conference On Acoustics, Speech And Signal Processing (ICASSP)*. IEEE, pp. 4580–4584.
- Schmidhuber, Jürgen (2015). “Deep Learning In Neural Networks: An Overview”. In: *Neural Networks* 61, pp. 85–117.
- Sermanet, Pierre and Yann LeCun (2011). “Traffic Sign Recognition With Multi-Scale Convolutional Networks”. In: *The 2011 International Joint Conference on Neural Networks*. IEEE, pp. 2809–2813.
- Sezer, Omer Berat, Mehmet Ugur Gudelek, and Ahmet Murat Ozbayoglu (2020). “Financial Time Series Forecasting With Deep Learning: A Systematic Literature Review: 2005–2019”. In: *Applied Soft Computing* 90, p. 106181.
- Shi, Xingjian, Zhourong Chen, Hao Wang, Dit-Yan Yeung, Wai-kin Wong, and Wang-chun Woo (2015). “Convolutional LSTM Network: A Machine Learning Approach For Precipitation Nowcasting”. In: *Advances In Neural Information Processing Systems* 28.
- Sirignano, Justin A. (2019). “Deep Learning For Limit Order Books”. In: *Quantitative Finance* 19.4, pp. 549–570.
- Sirignano, Justin A. and Rama Cont (2019). “Universal Features Of Price Formation In Financial Markets: Perspectives From Deep Learning”. In: *Quantitative Finance* 19.9, pp. 1449–1459.
- Stoll, Hans R. (1978). “The Supply Of Dealer Services In Securities Markets”. In: *The Journal of Finance* 33.4, pp. 1133–1151.
- Sutton, Rich (2019). *The Bitter Lesson*. URL: <http://www.incompleteideas.net/IncIdeas/BitterLesson.html>.
- Szegedy, Christian, Wei Liu, Yangqing Jia, Pierre Sermanet, Scott Reed, Dragomir Anguelov, Dumitru Erhan, Vincent Vanhoucke, and Andrew Rabinovich (2015). “Going Deeper With Convolutions”. In: *Proceedings Of The IEEE Conference On Computer Vision And Pattern Recognition*, pp. 1–9.
- Toth, Bence, Zoltan Eisler, Fabrizio Lillo, Julien Kockelkoren, Jean-Philippe Bouchaud, and J. Dooyne Farmer (2012). “How Does The Market React To Your Order Flow?” In: *Quantitative Finance* 12.7, pp. 1015–1024.
- Tran, Dat Thanh, Alexandros Iosifidis, Juho Kanninen, and Moncef Gabbouj (2019). “Temporal Attention-Augmented Bilinear Network For Financial Time-Series Data Analysis”. In: *IEEE Transactions On Neural Networks And Learning Systems* 30.5, pp. 1407–1418.
- Tsantekidis, Avraam, Nikolaos Passalis, Anastasios Tefas, Juho Kanninen, Moncef Gabbouj, and Alexandros Iosifidis (2017). “Forecasting Stock Prices From

- The Limit Order Book Using Convolutional Neural Networks”. In: *2017 IEEE 19th Conference on Business Informatics (CBI)*. Vol. 1. IEEE, pp. 7–12.
- (2020). “Using Deep Learning For Price Prediction By Exploiting Stationary Limit Order Book Features”. In: *Applied Soft Computing* 93, p. 106401.
- Vinyals, Oriol, Alexander Toshev, Samy Bengio, and Dumitru Erhan (2015). “Show And Tell: A Neural Image Caption Generator”. In: *Proceedings Of The IEEE Conference On Computer Vision And Pattern Recognition*, pp. 3156–3164.
- White, Halbert (1980). “A Heteroskedasticity-Consistent Covariance Matrix Estimator And A Direct Test For Heteroskedasticity”. In: *Econometrica* 48.4, pp. 817–838.
- Wilson, Andrew Gordon and Pavel Izmailov (2020). “Bayesian Deep Learning And A Probabilistic Perspective Of Generalization”. In: *arXiv preprint arXiv:2002.08791*.
- Wong, Bo K. and Yakup Selvi (1998). “Neural Network Applications In Finance: A Review And Analysis Of Literature (1990–1996)”. In: *Information & Management* 34.3, pp. 129–139.
- Xu, Ke, Martin D. Gould, and Sam D. Howison (2018). “Multi-Level Order-Flow Imbalance in a Limit Order Book”. In: *Market Microstructure and Liquidity* 04.03n04, p. 1950011.
- Zhang, Zihao, Bryan Lim, and Stefan Zohren (2021a). “Deep Learning For Market By Order Data”. In: *arXiv preprint arXiv:2102.08811*.
- Zhang, Zihao and Stefan Zohren (2021b). “Multi-Horizon Forecasting For Limit Order Books: Novel Deep Learning Approaches And Hardware Acceleration Using Intelligent Processing Units”. In: *arXiv preprint arXiv:2105.10430*.
- Zhang, Zihao, Stefan Zohren, and Stephen Roberts (2018). “BDLOB: Bayesian Deep Convolutional Neural Networks For Limit Order Books”. In: *arXiv preprint arXiv:1811.10041*.
- (2019a). “DeepLOB: Deep Convolutional Neural Networks for Limit Order Books”. In: *IEEE Transactions On Signal Processing* 67.11, pp. 3001–3012.
  - (2019b). “Extending Deep Learning Models For Limit Order Books To Quantile Regression”. In: *arXiv preprint arXiv:1906.04404*.